

1 **Current, steady-state and historical weathering rates of base**
2 **cations at two forest sites in northern and southern Sweden:**
3 **A comparison of three methods**

4 Sophie Casetou-Gustafson¹, Harald Grip², Stephen Hillier^{3, 5}, Sune Linder⁴, Bengt A.
5 Olsson¹, Magnus Simonsson⁵ Johan Stendahl⁵

6
7 ¹Department of Ecology, Swedish University of Agricultural Sciences, (SLU), P.O. Box 7044, SE-750 07
8 Uppsala, Sweden

9 ²Department of Forest Ecology and Management, SLU, SE-901 83 Umeå, Sweden. Present address:
10 Stjärnströms väg 5, SE-129 35 Hägersten, Sweden

11 ³The James Hutton Institute, Craigiebuckler, Aberdeen AB15 8QH, United Kingdom

12 ⁴Southern Swedish Forest Research Centre, SLU, P.O. Box 49, SE-230 53 Alnarp, Sweden

13 ⁵Department of Soil and Environment, SLU, P.O. Box 7014, SE-750 07 Uppsala, Sweden

14

15 *Correspondence to:* Sophie Casetou-Gustafson (Sophie.Casetou@slu.se)

16

17

18

19

20

21

22

23

24

25

26 **Abstract**

27 Reliable and accurate methods for estimating soil mineral weathering rates are required tools in evaluating the
28 sustainability of increased harvesting of forest biomass. A variety of methods that differ in concept, temporal and
29 spatial scale and data requirements are available for measuring weathering rates. In this study, release rates of
30 base cations through weathering were estimated in podsolised glacial tills at two experimental forest sites, Asa
31 and Flakaliden, in southern and northern Sweden, respectively. Three different methods were used: (i) historical
32 weathering since deglaciation estimated with the depletion method, using Zr as assumed inert reference; (ii)
33 steady-state weathering rate estimated with the PROFILE model, based on quantitative analysis of soil
34 mineralogy; and (iii) base cation budget at stand scale, using measured deposition, leaching and changes in base
35 cation stocks in biomass and soil over a period of 12 years.

36 In the 0–50 cm soil layer at Asa, historical weathering of Ca, Mg, K and Na estimated by the depletion
37 method was 4.7, 3.1, 0.8 and 2.0 mmol_c m⁻² yr⁻¹, respectively. Corresponding values at Flakaliden were 11.0, 12.9,
38 3.2 and 7.0 mmol_c m⁻² yr⁻¹, respectively. Steady state weathering rate for Ca, Mg, K and Na estimated with
39 PROFILE was 8.9, 3.8, 5.9 and 18.5 mmol_c m⁻² yr⁻¹, respectively, at Asa and 11.9, 6.7, 6.6 and 17.5 mmol_c m⁻²
40 yr⁻¹, respectively, at Flakaliden. At both sites, the PROFILE results indicated that steady-state weathering rate
41 increased with soil depth as a function of exposed mineral surface area, reaching a maximum rate at 80 cm (Asa)
42 and 60 cm (Flakaliden). In contrast, the depletion method indicated that the largest postglacial losses were in
43 upper soil layers, particularly at Flakaliden.

44 With the exception of Mg and Ca in shallow soil layers, PROFILE appeared to produce consistently higher
45 weathering rates than the depletion method, particularly of K and Na in deeper soil layers. In contrast, the
46 depletion method appeared to produce consistently lower rather than higher weathering rates, due to natural and
47 anthropogenic variability in Zr gradients. The base cation budget approach produced significantly higher
48 weathering rates of Ca, Mg, and K (65, 23, 40 mmol_c m⁻² yr⁻¹ at Asa and 35, 14 and 22 mmol_c m⁻² yr⁻¹ at Flakaliden),
49 but lower Na weathering rates similar to the depletion method (6.6 and 2.2 mmol_c m⁻² yr⁻¹ at Asa and Flakaliden).
50 The large discrepancy in weathering rates for Ca, Mg and K between the base cation budget approach and the
51 other methods suggest that there were additional sources for tree uptake in the soil besides weathering and
52 measured depletion in exchangeable base cations.

53

54 **Keywords.** Weathering; minerals; soil layers; nutrient mass-balance; *Picea abies*; PROFILE model; depletion;
55 base cation budget approach

56

57

58

59

60
61
62
63
64
65
66
67
68
69
70
71
72
73
74
75
76
77
78
79
80
81
82
83
84
85

Definitions and abbreviations

Mineralogy = The identity and stoichiometry of minerals present in a certain geographical unit, a particular site (*site-specific mineralogy*) or a larger geographical province (*regional mineralogy*)
Quantitative mineralogy or mineral composition = Quantitative information (wt.%) on the abundance of specific minerals in the soil.
Weathering rate = Weathering of a mineral resulting in release of a base cations per unit area per unit time.

Definitions:

$W_{\text{depletion}}$ = Historical weathering rate based on calculation of loss of mobile elements since last deglaciation
 W_{profile} = Steady-state weathering rate estimated using the PROFILE model
 W_{budget} = Current weathering rate based on base cation budget calculations

87 1. Introduction

88 Silicate weathering is the major long-term source of base cations in forest ecosystems (Sverdrup et al., 1988) and
89 is therefore crucial for sustainable plant production and for proton consumption, counteracting soil and water
90 acidification (Nilsson et al., 1982; Hedin et al., 1994; Likens et al., 1998; Bailey et al., 2003). These effects of
91 weathering are important in areas where in the past high sulphur (S) deposition has caused severe acidification of
92 forest soils and waters (Reuss and Johnson, 1986), for example in southern Scandinavia where felsic igneous
93 bedrock and less readily weatherable soils are abundant (Likens and Bormann, 1974). By 1990 in most European
94 countries, the trend of increasing S emissions since the 1950s started to abate (Grennfelt and Hov, 2005) and
95 forest and accumulation of base cations in tree biomass in excess of anion uptake has become a more important
96 source of acidity to the soil (Nilsson et al., 1982). Whole-tree harvesting can thus result in more acid, base cation-
97 depleted soils than stem-only harvesting (Olsson et al., 1996; Zetterberg et al., 2013). The combined effect of
98 increased productivity of forests in Sweden, resulting in increased stocks of forest biomass, and increased use of
99 whole-tree harvesting for energy purposes can therefore impede recovery from acidification and place increasing
100 demands on nutrient supply.

101 In society there is a need to know if current forestry practices are sustainable, that is if current weathering provides
102 enough base cations to at least balance their export by forestry. The role of weathering in maintaining base cation
103 balance in Swedish forest soils has been examined in several previous studies (Sverdrup and Rosén, 1998;
104 Akselsson et al., 2007). A regional-scale study on Swedish forest soils found that, in parts of Sweden, base cation
105 losses can occur at rates that lead to very low base saturation of the soils, possibly leading to negative effects on
106 e.g. soil fertility and runoff water quality within one forest rotation (Akselsson et al., 2007). Base cation depletion
107 in the soil was found to be more frequent after whole-tree harvesting than stem-only harvesting, especially for
108 Norway spruce, with deficits being more common in southern than in northern (boreal) Sweden.

109 In regional assessments of the sustainability of different harvesting regimes, the estimated weathering rate has a
110 strong influence on the base cation balance. Klaminder et al. (2011) found that different approaches to estimating
111 weathering rates yielded results that differed substantially, and that uncertainties in the methods had a great
112 influence on the predicted sustainability of different harvesting practices. Futter et al. (2012) compiled weathering
113 rates estimated at 82 sites, using different methods, and found both large between-site as well as within-site
114 differences in the values. Differences in input data can be attributed to different time scales used when acquiring
115 different input data, challenges determining accurate mineralogical compositions and the use of field data
116 compared with laboratory data (Van der Salm, 2001; Futter et al., 2012). Thus, they recommend that at least three
117 different approaches be applied per study site to evaluate the precision in weathering estimates. The approaches
118 examined in the present paper include (1) 'historical weathering' based on geochemical investigation of the soil
119 profile, (2) modelled present weathering rate and (3) present weathering rate based on cation balances at the
120 ecosystem level. The choice of methods is primarily based on the fact that rates of weathering may vary over time
121 (Klaminder et al., 2011; Stendahl et al., 2013). The average weathering under long-term environmental change,
122 i.e. 'historical weathering', is thus different from the weathering potential under present-day environmental

123 conditions, i.e. ‘present-day weathering’, which is why we need to be able to consider historical weathering when
124 assessing current/present-day weathering rates. Moreover, present-day weathering rates estimated based on the
125 steady-state concept, which lacks the dimension of time, may differ from dynamic estimates of weathering rates
126 derived from measured base cation budgets. These three different concepts of estimating weathering cannot be
127 covered by a single method (Klaminder et al., 2011; Futter et al., 2012). Weathering estimates based on these
128 concepts have often differed largely from pedon to catchment scale, whereas truly harmonized comparisons of
129 methods require that methods are tested uniformly at the same spatial scale. This spatial scale can be the pedon,
130 which also contains the major part of the mineral nutrient sources in the soil available for forest growth. To our
131 knowledge, Kolka et al. (1996) is the only study to have previously used this approach.

132

133 The first approach, the depletion method, makes use of soil profile based mass balances (Chadwick et al., 1990;
134 Brimhall et al., 1991) to estimate total base cation losses in the soil above a reference soil depth. An element in a
135 weathering-resistant mineral is used as a standard, most commonly zirconium (Zr, present in e.g. zircon) or
136 titanium (Ti, present in e.g. rutile) (Sudom and St.Arnaud, 1971; Harden et al., 1987; Chadwick et al., 1990; Bain
137 et al., 1994), due to their stability at low temperatures (Schützel et al., 1963). To yield an annual average
138 weathering rate ($\text{mmol}_c \text{m}^{-2}$), calculated element losses are commonly divided by an estimated soil age. In Nordic
139 glacial tills situated above the marine limit, soil age is conventionally considered to be the number of years lapsed
140 since the site of interest was finally deglaciated at the end of the Weichselian. Since the rate of weathering may
141 vary over time (Klaminder et al., 2011; Stendahl et al., 2013), the average ‘historical weathering’ rate may differ
142 from the present-day weathering rate. The depletion method is most widely used in Sweden to estimate weathering
143 rates, specifically at the regional scale (Olsson et al., 1993).

144

145 The second approach commonly involves the mechanistic PROFILE model, by which release rates of base cations
146 are estimated based on the dissolution kinetics of a user-defined set of minerals present in the soil, and the physical
147 and chemical conditions that drive the dissolution of minerals. Since it is a mechanistic model, its strength is its
148 transparency, while its main weakness is the difficulty in setting values of model parameters and input variables
149 to which it may have high sensitivity. Akselsson et al. (*this issue*) concluded that the most important way to reduce
150 uncertainties in modelled weathering rates is to reduce input data uncertainties, e.g. regarding soil texture,
151 although there is still a need to improve process descriptions of e.g. biological weathering and weathering brakes
152 (e.g. Erlandsson Lampa et al., *this issue*). The sensitivity of PROFILE to variations in soil physical parameters
153 (e.g. soil texture, soil bulk density) and mineral composition was discussed by Jönsson et al. (1995) and Hodson
154 et al. (1996), while the importance of the ability to determine the precise identity and quantity of the minerals was
155 analysed by Casetou-Gustafson et al. (*this issue*).

156

157 The third approach to estimating weathering rate is the base cation budget approach (Velbel, 1985; Likens et al.,
158 1998). This method has been applied to estimate current weathering rates at various temporal and spatial scales,
159 and components of the budget approach have been used in different ways in some models, e.g. MAGIC (Cosby
160 et al., 1985). The weathering rate is estimated indirectly as the difference between other sinks and sources of base
161 cations, which are measured within a system with defined boundaries. The missing source in the mass balance

162 equation is assumed to represent the weathering. The base cation budget approach is most reliable when based on
163 long-term data from well-defined systems, although even then estimated weathering rates suffer from large
164 uncertainties, as errors in the sinks and sources accumulate in the mass balance equation (Simonsson et al., 2015).
165 The base cation budget approach has mostly been applied under conditions where accumulation in biomass were
166 not directly measured but estimated to be small, or base cation stocks in the soil were assumed to be at steady-
167 state (e.g. Kolka et al., 1996; Sverdrup et al., 1998; Whitfield et al., 2006). Consequently, at the pedon scale, the
168 PROFILE model and the depletion method are the most frequently used methods in Sweden to estimate
169 weathering rates.

170 In this study, we applied the three conceptually different methods of estimating weathering on two well-defined
171 forest ecosystems, Asa and Flakaliden in southern and northern Sweden, to allow a harmonized comparison of
172 methods, and to place weathering in the context of other base cation fluxes in aggrading Norway spruce forests.
173 The base cation budgets were estimated at the period of stand development when nutrient demand was expected
174 to peak. In combination with access to highly accurate data on biomass production, these conditions also provided
175 opportunities to relate weathering to base cation accumulation in biomass at high nutrient uptake rates, and
176 possible simultaneous depletions of extractable base cation stocks in the soil. Furthermore, input data to PROFILE
177 were characterised by high quality quantitative mineralogical data, measured directly by X-ray powder diffraction
178 (XRPD), as previously discussed by Casetou-Gustafson et al. (2018).

179 Three test criteria were used to examine the outputs of the depletion method and PROFILE model: (1) similarity
180 in weathering estimates for the 0-50 cm soil profile; (2) similarity in depth gradients in weathering for the 0-100
181 cm soil profile; and (3) similarity in ranking order of the base cations released.

182 **2. Materials and methods**

183 **2.1 Study sites**

184 Two forest sites planted with Norway spruce (*Picea abies* (L.) Karst) were chosen for the study, Flakaliden in
185 northern Sweden (64°07'N, 19°27'E) and Asa in southern Sweden (57°08'N, 14°45'E), because they have been
186 used for long-term experimental studies on the effects of climate and nutrient and water supply on tree growth
187 and element cycling (Linder, 1995; Bergh et al., 1999; Ryan, 2013).

188
189 The experiment at Flakaliden was established in 1986 in a 23-year-old Norway spruce stand, planted in 1963 with
190 four-year-old seedlings of local provenance after prescribed burning and soil scarification (Bergh et al., 1999).
191 The experiment at Asa was established one year later (1987), in a 12-year-old Norway spruce stand planted in
192 1975 with two-year-old seedlings after clear-felling and soil scarification. The experimental design was similar at
193 both sites and included control, irrigation and two nutrient optimisation treatments (Bergh et al., 1999). All
194 treatments were replicated in 50 m x 50 m plots, arranged in a randomised block design. Only two of the four
195 treatments were used in the present study; the control (C) and plots receiving an annual dose of an optimised mix
196 of solid fertiliser (F), which among other elements per year contained about 10 kg ha⁻¹ Ca, 8 kg ha⁻¹ Mg and 45
197 kg ha⁻¹ K (Linder, 1995).

198

199 Flakaliden is located in the central boreal sub-zone with a harsh climate, with long cool days in summer and short
200 cold days in winter. Mean annual temperature for the period 1990-2009 was 2.5 °C, and mean monthly
201 temperature varied from -7.5 °C in February to 14.5 °C in July. Mean annual precipitation in the period was ~650
202 mm, with approximately one-third falling as snow, which usually covers the frozen ground from mid-October to
203 early May. Mean length of the growing season (daily mean temperature ≥ 5 °C) was 148 days, but with large
204 between-year variations (Table 1) (cf. Sigurdsson et al., 2013).

205

206 Asa is located in the hemi-boreal zone, where the climate is milder than at Flakaliden, which is reflected in a
207 longer growing season (193 days). Mean annual temperature (1990-2009) was 6.3 °C, mean monthly temperature
208 varied from -1.9 °C in February to 16.0 °C in July and mean annual precipitation was ~750 mm. The soil is
209 periodically frozen in winter. The difference in climate is reflected in differences in site productivity, which
210 broadly follows climate gradients in Sweden (Bergh et al., 2005).

211

212 The soils at Asa and Flakaliden differ in age due to differences in the time since deglaciation (Table 1), from
213 approximately 14,300 years at Asa and 10,150 years at Flakaliden (estimated from Fredén, 2009). The soil type
214 at both sites is an Udic Spodosol, with a mor humus layer overlying glacial till derived from felsic bedrock. The
215 soil texture is classified as sandy loam. The transition between the B- and C-horizons is mostly located at 50 cm
216 depth at Flakaliden and 50-60 cm depth at Asa. The natural ground vegetation at Flakaliden is dominated by
217 *Vaccinium myrtillus* (L.) and *V. vitis-idaea* (L.) dwarf-shrubs, lichens and mosses (Kellner, 1993; Strengbom et
218 al., 2011). The ground vegetation at Asa is dominated by *Deschampsia flexuosa*, (L.) and mosses (Strengbom et
219 al., 2011; Hedwall et al., 2013).

220 **2.2. Soil sampling and analyses of geochemistry and mineralogy**

221 A detailed description of soil sampling, geochemical analyses and determination of mineralogy can be found in
222 Casetou-Gustafson et al. (2018). The procedures are summarised below.

223 Sampling was performed in untreated control plots (K1 and K4 at Asa and 10B and 14B at Flakaliden) and
224 fertilised (F) plots (F3, F4 at Asa and 15A and 11B at Flakaliden) in October 2013 (Flakaliden) and March 2014
225 (Asa), in the border zone of four plots at each site. One intact soil core per plot at Flakaliden and in plot K1 at Asa
226 was extracted using a rotary drill (17 cm inner diameter). In plots K4, F3 and F4 at Asa, soil samples were instead
227 taken from 1 m deep manually dug soil pits, due to inaccessible terrain for the rotary drill machinery. Maximum
228 soil depth was shallower at Flakaliden (70-90 cm) than at Asa (90-100 cm). The volume of stones and boulders
229 was determined for each plot at the two study sites using the penetration method described by Viro (1952) to a
230 maximum depth of 30 cm and by applying the fitted function described by Stendahl et al. (2009). Mean stone and
231 bolder content was higher at Flakaliden (39%_{vol}) than at Asa (28%_{vol}).

232 Soil samples were taken from each 10-cm soil layer. Prior to chemical analysis, these samples were dried at 30-
233 40 °C and sieved to <2 mm. Analysis of particle size distribution was performed by wet sieving and sedimentation

234 (pipette method) in accordance with ISO 11277. Geochemical analyses were conducted by ALS Scandinavia AB
235 and comprised inductively coupled plasma-mass spectrometry (ICP-MS) on HNO₃ extracts of fused samples that
236 were milled and ignited (1000 °C) prior to fusion with LiBO₂.

237 Quantitative soil mineralogy was determined with the X-ray powder diffraction (XRPD) technique (Hillier 1999,
238 2003). Samples for measurement of XRPD patterns were prepared by spray drying slurries of soil samples (<2
239 mm) micronised in ethanol. A full pattern fitting approach was used for quantitative mineralogical analysis of the
240 diffraction data (Omotoso et al., 2006). This fitting process involved the modelling of the measured diffraction
241 pattern as a weighted sum of previously measured and verified standard reference patterns of the identified mineral
242 components. The determination of chemical compositions of various minerals present in the soils was conducted
243 by electron microprobe analysis (EMPA) of mineral grains subsampled from the sifted (< 2 mm) soil samples.

244 **2.3 Historical weathering determined with the depletion method**

245 **2.3.1 Method description**

246 The depletion method (Table 2), as defined by Marshall and Haseman (1943) and Brimhall et al. (1991), estimates
247 the accumulated mass loss since soil formation (last deglaciation for our sites) as a function of loss of a mobile
248 (weatherable) element and enrichment of an immobile (weathering resistant) element according to the following
249 general function introduced by Olsson and Melkerud (1989) and based on the same theories as the mass transfer
250 function described in Brimhall et al. (1991):

$$251 \quad W_{\text{depletion},i} = \frac{d \cdot \rho}{100} \cdot \frac{X_c \cdot Zr_{w,i}}{Zr_c} - X_{w,i} \quad (1)$$

252 where W denotes loss of the i th element (g m⁻²), X denotes mobile element concentrations (%), Zr denotes
253 immobile element concentrations (%), w and c denote a weathered soil layer and the assumed unweathered
254 reference layer, respectively, d is layer thickness (m), and ρ is bulk density (g m⁻³). Zirconium is commonly used
255 as the immobile element due to the inert nature of the mineral zircon (ZrSiO₄), although Ti is sometimes used due
256 to the resistance of the Ti-containing minerals anatase and rutile (TiO₂) to weathering (Olsson and Melkerud,
257 1989). The unweathered reference layer is located in the C horizon, and has X to Zr ratios that are assumed to
258 represent pristine conditions of the presently weathered layers above it. In the weathered layers, X to Zr ratios are
259 smaller; that is, Zr is enriched compared with the mobile elements (i.e. the base cations). The method is based on
260 the assumptions that Zr, hosted in zircon, was uniformly distributed throughout the soil profile at the time of
261 deglaciation, that weathering only occurs above the reference layer and that zircon does not weather. The latter
262 implies that Zr concentrations and Zr/base cation ratios are constant below the reference layer. Table 3 shows the
263 reference depths for different base cations compared with Zr, which were used as the depths of immobile element
264 concentrations. The Zr/base cation ratio (Fig. S3) was used to help select the reference soil layer as it highlights
265 heterogeneities in parent material with depth. In cases of heterogeneities in the profile, the reference layer was
266 chosen above this heterogeneity. This choice was precluded for soil profile 11B, where Zr concentrations and
267 Zr/base cation ratios peaked directly below the B-horizon (i.e. at 50-60 cm).

268 2.3.2. Application

269 Prior to calculating base cation weathering rates with the depletion method, fractional volume change (Vp) was
270 calculated according to White et al. (1996) in order to assess if there were any large volume changes (collapse)
271 in the mineral soil with implications for which depth the weathering should be calculated to. Similar to White et
272 al. (1996), it was assumed that values close to zero indicate no volumetric change, which was the case below 30-
273 40 cm of soil depth at both sites (Table S5). The homogeneity of the parent material was also evaluated (Fig. 1)
274 using the criterion that the ratio of Ti to Zr should be more or less stable with depth in an originally homogeneous
275 material. Use of the ratio of two immobile elements to establish uniformity of parent material has been suggested
276 previously (Sudom and St.Arnaud, 1971; Starr et al., 2014). The homogeneity criterion was not met using Zr in
277 plot K1 at Asa (i.e. the Zr concentrations decreased towards the soil surface; Fig. 2); here Ti was used as the
278 immobile element instead. Furthermore, the plots 15A and 11B at Flakaliden had to be eliminated from the
279 calculations, because relatively large variability in both the Zr and Ti gradients was observed. These large
280 heterogeneities led to an overall gain of base cations in the rooting zone, which is opposite to what would be
281 expected (i.e. that losses and gains can occur at specific soil depths due to eluviation and illuviation processes in
282 podzolic soils). For this reason, soil profiles 15A and 11B were eliminated from further consideration in
283 calculations of historical weathering rates using the depletion method. Thus, apart from heterogeneities,
284 transportation processes (eluviation and illuviation) and/or erratic Zr or Ti gradients could lead to “negative”
285 weathering, i.e. leading to a calculated relative accumulation of elements. Such negative values were not
286 considered in the calculation of historical weathering losses.

287 Bulk density was estimated for each soil layer except in some plots where density measurements could not be
288 made below a certain soil depth. Bulk density in these cases was estimated using an exponential model for total
289 organic carbon (TOC) and bulk density (BD, g/cm^3) based on our own data. For Asa (soil layers F3: 70-90 cm;
290 F4: 0-10, 30-40, 50-60, 60-70, 70-80, 80-90, 90-100 cm; and K4: 70-80, 80-90, 90-100 cm), the following function
291 was used:

$$292 \rho = 1.3 e^{-0.1 x} \quad (2)$$

293 where x is TOC content (% of dry matter).

294 For Flakaliden (soil layers 14B: 80-90cm; 10B: 60-70 cm; and 11B: 40-70 cm), the function used was:

$$295 \rho = 1.8 e^{-0.2 x} \quad (3)$$

296 2.4 The PROFILE model

297 2.4.1 Model description

298 The steady state weathering of soil profiles was estimated using the biogeochemical PROFILE model (Table 2),
299 where weathering of the i th base cation ($W_{\text{profile}, i}$) is described by long-term mineral dissolution kinetics at the
300 interface of wetted mineral surfaces and the soil solution. PROFILE is a multilayer model, where parameters are
301 specified for each soil layer based on field measurements and estimation methods (Warfvinge and Sverdrup,
302 1995).

303 **2.4.2 PROFILE parameter estimation**

304 A detailed description of the application of the PROFILE model to the soils and sites in the present study can be
305 found in Casetou-Gustafson et al. (*this issue*). The parameters used are listed in Table 4.

306 Exposed mineral surface areas were estimated from soil bulk density and texture data using the algorithm specified
307 in Warfvinge and Sverdrup (1995). Volumetric soil water content for each soil profile in Flakaliden and Asa was
308 estimated to be $0.25 \text{ m}^3 \text{ m}^{-3}$ according to the moisture classification scheme described in Warfvinge and Sverdrup
309 (1995) (Table S4).

310 The aluminium (Al) solubility coefficient, a soil chemical parameter needed for solution equilibrium reactions,
311 was defined as $\log\{\text{Al}^{3+}\}+3\text{pH}$. It was estimated by applying a function developed from previously published data
312 (Simonsson and Berggren, 1998) and existing total carbon and oxalate-extractable Al measurements for our sites
313 (Casetou-Gustafson et al., 2018) (Table S4). For partial CO_2 pressure in the soil, the default value of Warfvinge
314 and Sverdrup (1995) was used. Data on measured dissolved organic carbon (DOC) in the soil solution at 50 cm
315 depth were available for plots K4 and K1 at Asa and plots 10B and 14B at Flakaliden, and these values were also
316 applied for deeper soil horizons. Shallower horizons (0-50 cm) were characterised by higher DOC values, based
317 on previous findings (Fröberg et al., 2006, 2013) and the DOC classification scheme in Warfvinge and Sverdrup
318 (1995) (Table S4).

319 The site-specific parameters used were evapotranspiration, temperature, atmospheric deposition, precipitation,
320 runoff and nutrient uptake in biomass (Table 4). Mean evapotranspiration per site was estimated from mean annual
321 precipitation and runoff data, using a general water balance equation.

322 Total deposition was calculated using deposition data from two sites of the Swedish ICP Integrated Monitoring
323 catchments, Aneboda (for Asa) and Gammtratten (for Flakaliden) (Löfgren et al., 2011). Na was used as a tracer
324 ion in order to distinguish canopy exchange from dry deposition for Ca, Mg and K. Dry deposition for Na and Cl
325 was calculated as the difference between wet and throughfall deposition. As outlined in Zetterberg et al. (2016),
326 wet deposition for all elements was calculated by correcting bulk deposition for dry deposition using wet-only to
327 bulk deposition ratio. Wet deposition was estimated based on the contribution of dry deposition to bulk deposition,
328 both for base cations and anions, using dry deposition factors from Karlsson et al. (2012,2013). Finally, total
329 deposition for all elements was calculated from the sum of dry and wet deposition.

330 Net base cation and nitrogen uptake in aboveground tree biomass (i.e. bark, stemwood, living and dead branches,
331 needles) was estimated as mean accumulation rate over a 100-year rotation period in Flakaliden and a 73-year
332 rotation period in Asa. These calculations were based on Heureka simulations using the StandWise application
333 (Wikström et al., 2011) for biomass estimates, in combination with measured nutrient concentrations in
334 aboveground biomass as described in section 2.5.4 below (Linder, unpubl. data).

335 **2.4.3 PROFILE sensitivity analysis**

336 The sensitivity of PROFILE to changes in soil physical and mineralogical input was analysed, to test to what
337 extent the depth gradients of weathering rates as predicted by PROFILE were affected primarily by soil physical
338 properties or by soil mineralogy. Independent PROFILE runs were performed, after replacing horizon-specific
339 input values with soil profile average values regarding either (1) soil bulk density and specific exposed mineral
340 surface area ('homogenous soil physics'), or (2) soil mineral percentages ('homogenous mineralogy'), or (3) both
341 ('homogenous soil physics and mineralogy'). In each scenario, the squared deviation in weathering rate was
342 calculated for each base cation and horizon, compared to the normal simulation based on horizon-specific inputs
343 for soil physics and soil mineralogy. The sum of squares over base cations and horizons was used as a measure of
344 the overall error caused by the 'homogenous' input data. The ratios of sum of squares, of scenario (1) over (3)
345 and of scenario (2) over (3), was used to estimate the percent contribution of soil physics and soil mineralogy,
346 respectively, to the overall weathering gradients in the soil profile.

347 **2.5 The base cation budget approach**

348 **2.5.1. General concepts of the base cation budget approach**

349 The average weathering rate of the i th base cation according to base cation budget, $W_{\text{budget}, i}$, over a period of time
350 can be estimated with base cation budgets (Table 2) using the base cation budget approach, which assumes that
351 total deposition (TD_i) and weathering are the major sources of mobile and plant-available base cations in the soil,
352 and that leaching (L_i) and accumulation of base cations in biomass (ΔB_i) are the major sinks. A change in the
353 extractable soil stocks of base cations over time (ΔS_i) are considered as a sink if stocks have increased, or as a
354 source if stocks have been depleted (Simonsson et al., 2015). Each of these terms is measured independently over
355 a specific period of time. Hence,

$$356 \quad W_{\text{budget}, i} = L_i + \Delta B_i + \Delta S_i - TD_i \quad (4)$$

357 **2.5.2 Atmospheric deposition, TD_i**

358 The same estimates of total atmospheric deposition as used in parameter setting of the PROFILE model (section
359 2.4.2) were used in the base cation budget, Eq. (4).

360 **2.5.3. Changes in exchangeable soil pools, ΔS_i**

361 Changes in extractable base cation stocks in the soil were calculated from the difference between two soil
362 samplings, performed in 1986 and 1998 at Flakaliden, and in 1988 and 2004 at Asa. The organic layer was sampled
363 with a 5.6 cm diameter corer, whereas a 2.5 cm diameter corer was used to sample 10 cm sections to 40 cm depth
364 in the mineral soil. For each plot and layer, 25 cores were combined into one sample.

365

366 Exchangeable base cation content in the soil (<2 mm) all Flakaliden samples in Asa samples from 1988 was
367 determined by extraction of dry samples with 1 M NH_4Cl using a percolation method, where 2.5 g of sample was
368 leached with 100 mL of extractant at a rate of 20 mL h^{-1} . The base cations were analysed by atomic absorption
369 spectrophotometry (AAS). For the Asa samples from 2004, batch extraction was performed using the same

370 extractant, and the base cations were determined with ICP. A separate test was made to compare the yield of the
371 percolation and batch extraction methods. No consistent difference between the methods was observed.

372

373 The amount of fine soil (<2 mm) per unit area was calculated from the volume of fine earth (<2 mm) in the soil
374 profiles and the average bulk density of the soil in the 0-10, 10-20 and 20-40 cm layers. Bulk density and volume
375 proportion of stoniness at Flakaliden were determined from samplings in 1986 in 20 soil profiles (0.5 m x 0.5 m
376 and about 0.5 m deep) outside plots. At Asa, stoniness was determined with the penetration method of Stendahl
377 et al. (2009) and the bulk density of soil <2 mm was calculated using a pedotransfer function that included soil
378 depth and measured carbon concentrations as variables.

379 **2.5.4 Net uptake in biomass, ΔB_i**

380 Accumulation of base cations in tree biomass, i.e. net uptake of base cations, was calculated as a mean value of
381 control plots over the period 1989-2003, based on increments in aboveground biomass at Asa and Flakaliden for
382 this period and on the concentrations of elements in different tree parts. The increment in aboveground biomass
383 was based on measurements of stem diameter at breast height (DBH) of all individual trees in the plots, and
384 applying DBH data to allometric functions developed for Norway spruce at the sites (Albaugh et al., 2009, 2012).
385 The allometric functions were based on destructive samplings (1987 - 2003) of 93 and 180 trees at Asa and
386 Flakaliden respectively. The increment in belowground biomass was estimated from general allometric functions
387 for Norway spruce stumps and roots in Sweden (Marklund, 1988). Since Marklund's functions (1988)
388 underestimate belowground biomass by 11%, a factor to correct for this was included (Pettersson and Ståhl, 2006).
389 Furthermore, the finest root fraction (≤ 2 mm), which is not included in the functions of Marklund (1988) and
390 Pettersson and Ståhl (2006), was assumed to be 20% of needle biomass at Asa and 33% at Flakaliden, respectively,
391 based on data from Helmisaari et al. (2007).

392

393 Data on element concentrations in biomass were available from measurements on harvested trees (S. Linder,
394 unpublished data). At Flakaliden, total element concentrations were analysed in trees sampled for biomass
395 determination in 1992 and 1997. Analyses of needles and branches (dead and live) were conducted on the same
396 tree parts in the biomass sampled in 1993 and 1998. Base cation concentrations in biomass were determined from
397 acid wet digestion in HNO_3 and HClO_4 , followed by determination of elements by ICP-atomic emission
398 spectrophotometry (ICP-AES) (Jobin Yvon JY-70 Plus).

399

400 Data on element concentrations in belowground biomass fractions were taken from literature from the Nordic
401 countries (Hellsten et al., 2013). Specifically, data on stump and root biomass of Norway spruce were available
402 for Asa and data from Svartberget was used for Flakaliden (Table 7 in Hellsten et al., 2013).

403 **2.5.5. Leaching, L_i**

404 Base cation leaching was quantified in six-month intervals from modelled daily runoff multiplied by average
405 element concentrations in soil water collected with tension lysimeters at 50 cm soil depth.

406

407 Soil water was collected from five ceramic tension lysimeters (P80) installed at 50 cm depth in each experimental
408 plot. Soil water was collected during frost-free seasons, applying an initial tension of 70 kPa in 250 mL sampling
409 bottles, and left overnight. These soil water samples were pooled by plot. The base cation concentration in the soil
410 solution was determined with ICP-AES. Soil water sampling was performed twice every year, i.e. in the spring
411 and in the autumn, which are the periods of highest water flux and which means that the most important leaching
412 events were covered. The spring samples were collected soon after the snowmelt and depending on the weather
413 in a specific year this meant that the yearly spring sampling date varied between the last week of April and the
414 last week of May. The autumn samples were collected when frost risk increased. That meant that the autumn
415 sampling dates varied from year to year, i.e. from the first week in September to mid-November. The seasonal
416 variation in soil water chemistry is shown in Fig. S4).

417

418 The drainage flux out of the profile was calculated by the CoupModel (Jansson, 2012). The model was
419 parameterised based on hydraulic soil properties measured at the sites. The model was run with hourly mean
420 values of locally measured climate variables (precipitation, global radiation, wind speed, air temperature and
421 humidity) and model outcomes were tested against tensiometer data, i.e. bi-weekly tensiometer readings at 15, 30
422 and 45 cm depth were used for model calibration. The parameters were then adjusted slightly to obtain good
423 agreement between measured and calculated soil water content. Annual precipitation varied considerably during
424 the period 1990-2002, ranging from 906 to 504 mm at Flakaliden (mean 649 mm) and from 888 to 575 mm at
425 Asa (mean 736 mm). Annual evapotranspiration increased by about 50 mm at both sites, during the period 1987-
426 2003 at Flakaliden and 1990-2002 at Asa, due to the increment in tree leaf area. Monthly means and standard
427 deviation of drainage (mm) at 50 cm depth in the soil of control plots at Asa during 1990 – 2004 and at Flakaliden
428 during 1988-2004 are shown in Fig. S5.

429 **2.5.6. Assessment of data quality in base cation budget**

430 The precision and accuracy of a base cation budget estimate of $W_{\text{budget}, i}$ was determined by the quality of estimates
431 of each individual term in Eq. (3), in proportion to the magnitude of each term (Simonsson et al., 2015). Significant
432 uncertainty in the estimate of a quantitatively important term will therefore dominate the overall uncertainty in
433 estimates of W_{budget} . Firstly, the quality of data for each term in Eq. (3) was assessed based on the spatial and
434 temporal scales of measurements and the quality of measurements (Table 5). Using these criteria, we consider the
435 estimates of deposition, leaching and accumulation in biomass to be of moderate to high quality. The
436 measurements of changes in extractable soil pools were of lower quality because extraction methods were not
437 identical for samples collected 1986/1988 and 1998/2004, which would cause significant uncertainty if soil
438 changes were an important part of the element budget. To partly overcome this uncertainty, we used the estimates
439 obtained by the PROFILE ($W_{\text{profile}, i}$) and depletion method ($W_{\text{depletion}, i}$) in additional base cation budget calculations
440 where the change in soil was determined from the base cation budget. These additional base cation budget
441 estimates, which are conceptually analogous to the regional mass balances presented by Akselsson et al. (2007),
442 were also used to place the PROFILE and depletion method estimates of W_i in the context of other base cation
443 fluxes at the ecosystem scale.

444

445 2.6 Statistical analyses

446 Site mean values and standard error (SE) of $W_{\text{depletion}}$, W_{profile} were calculated based on the four (or two) soil profiles
447 studied at each site. For W_{budget} an average based on the four control plots at each site was calculated as well as a
448 combined standard uncertainty. The latter was partly based on standard errors derived from plot-wise replicated
449 data of the present experiments (for leaching and changes in exchangeable soil pools, $SE(L_i)$ and $SE(\Delta S_i)$,
450 respectively), partly on standard uncertainties (u) derived from Simonsson et al. 2015, where replicated data were
451 missing in the present study (for accumulation in biomass and total deposition, $u(\Delta B_i)$ and $u(TD_i)$, respectively).
452 Because total deposition and bioaccumulation differed substantially from those in the study of Simonsson et al.
453 2015, relative standard uncertainties were derived from that study, and multiplied with the average deposition and
454 bioaccumulation rates at Asa and Flakaliden, respectively, to yield realistic standard uncertainties for the present
455 sites. For the weathering rate of the i th base cation according to Eq. (4), a combined standard uncertainty (u_c) was
456 calculated as:

$$457 \quad u_c(W_{\text{budget}, i}) = \sqrt{(SE(L_i))^2 + (u(\Delta B_i))^2 + (SE(\Delta S_i))^2 + (u(TD_i))^2} \quad (5)$$

458 Confidence intervals were calculated by multiplying the combined standard uncertainties with a coverage factor
459 of 3.

460

461 3. Results

462 3.1 Depletion method estimates of historical weathering rates

463 At both Asa and Flakaliden, historical weathering rates estimated with the depletion method ($W_{\text{depletion}}$) were
464 highest in the upper soil layers and showed a gradual decrease down to the reference depth, which was defined at
465 60-70 cm at Flakaliden and for most plots at 80-90 cm at Asa (Fig. 3). Flakaliden had a higher historical annual
466 weathering rate to 90 cm soil depth, $37.8 \text{ mmol}_c \text{ m}^{-2}\text{yr}^{-1}$, than Asa, $12.8 \text{ mmol}_c \text{ m}^{-2}\text{yr}^{-1}$; the corresponding value
467 for 0-50 cm depth was $34.1 \text{ mmol}_c \text{ m}^{-2}\text{yr}^{-1}$ at Flakaliden and $10.5 \text{ mmol}_c \text{ m}^{-2}\text{yr}^{-1}$ at Asa. The gradients with depth
468 showed that $W_{\text{depletion}}$ increased towards the surface, although this trend was more pronounced at Flakaliden than
469 at Asa. At Flakaliden, $W_{\text{depletion}}$ was highest for Mg, followed by Ca, Na and K (Figs. 3 and 4); at Asa, it was
470 highest for Ca, closely followed by Mg, Na and K (Figs. 3 and 4).

471 3.2 PROFILE model estimates of steady state weathering rates

472 The steady state weathering rate estimated by the PROFILE model (W_{profile}) differed from the historical rate with
473 respect to all three test criteria, i.e. (1) total weathering rate in the 0-50 cm soil layer, (2) variation in weathering
474 with depth and (3) ranking order of base cations (Figs. 3 and 4). Firstly, regarding base cation weathering rate in
475 the upper 50 cm of the mineral soil, W_{profile} estimates for Asa and Flakaliden (Asa: $37.1 \text{ mmol}_c \text{ m}^{-2}\text{yr}^{-1}$, Flakaliden:
476 $42.7 \text{ mmol}_c \text{ m}^{-2}\text{yr}^{-1}$) were around 3.5 and 1.3-fold higher than $W_{\text{depletion}}$ estimates, respectively. Secondly, the total

477 modelled base cation weathering rate for the soil profile down to 90 cm was around 7-fold higher than the rate
478 estimated using the depletion method at Asa ($89.4 \text{ mmol}_e \text{ m}^{-2}\text{yr}^{-1}$), and 3.4-fold higher at Flakaliden (127.6 mmol_e
479 $\text{m}^{-2}\text{yr}^{-1}$). Unlike the historical weathering based on the depletion method, PROFILE predicted that weathering
480 rates increased with soil depth at both sites. At Flakaliden, high contents of K- and Mg-bearing tri-octahedral mica
481 (Casetou-Gustafson et al., 2018) gave rise to particularly high weathering rates at 70-80 cm. Thirdly, as opposed
482 to $W_{\text{depletion}}$, W_{profile} was largest for Na at both sites, followed by Ca. However, W_{profile} was larger for K than for Mg
483 at Asa, while the reverse was true at Flakaliden.

484 The sensitivity analysis of the PROFILE model using homogeneous soil physical and/or mineralogical properties
485 demonstrated that the variations in soil physical properties (i.e. soil bulk density and specific exposed mineral
486 surface area) with depth had a greater influence than mineralogy on the observed change in W_{profile} with soil depth.
487 In terms of the ratios of sums of squares, the ‘homogenous soil physics’ of scenario (1) produced 75% or more of
488 the error obtained with ‘homogenous soil physics and mineralogy’ (scenario (3)), leaving a mere 25% or less to
489 the ‘homogenous mineralogy’ of scenario (2); also see Tables S1 and S2. The soil physical inputs that were more
490 important for PROFILE weathering rates are indicated in Figs. S1 and S2. There was a strong linear and positive
491 relationship between exposed mineral surface area and W_{profile} for all elements at both sites, with R^2 values ranging
492 from 0.65 to 0.89 (Fig. S1). The relationship between bulk density and W_{profile} was also strong and showed the
493 same linear response, although R^2 values were lower, 0.40-0.70 (Fig. S2).

494 3.3 Base cation budget estimates of current weathering rates

495 A comparison of weathering rates estimated by base cation budgets (W_{budget}), W_{profile} and $W_{\text{depletion}}$ was made for
496 the 0-50 cm soil layer. It was found that, for most elements, W_{budget} in the 0-50 cm layer was higher, or much
497 higher, than W_{profile} (Fig. 4). Compared with the PROFILE model estimates, the base cation budget estimates of
498 weathering were 6- to 7-fold higher for Ca, Mg and K weathering at Asa, and about 2- to 3-fold higher for Ca,
499 Mg and K at Flakaliden. At Asa, the sum of base cations was on average 13-fold and 3.6-fold larger than $W_{\text{depletion}}$
500 and W_{profile} , respectively. The closest resemblance between methods was found between $W_{\text{depletion}}$ and W_{budget} for
501 Na. The budget calculations suggested that weathering was a dominant source of K and Mg, but contributed a
502 somewhat smaller proportion of Ca (61% at Asa and 43% at Flakaliden).

503

504 As to the fluxes (terms) of the base cation budget, Na showed patterns different from those of K, Mg and Ca (Fig.
505 5). For Na, uptake in biomass was negligible and leaching was the dominant sink. For the latter three elements,
506 accumulation in biomass was the dominant sink. Loss by leaching was negligible for K, but significant for Mg
507 and Na. Deposition generally represented only a small input, except for Na at Asa. The measured decreases in soil
508 stocks of exchangeable base cations indicated that a change in this pool was a particularly important source of Ca.
509 There were minor increases in exchangeable stocks for Na, K and Mg at Asa. The combined uncertainty of W_{budget}
510 was larger for Ca and K, both dominated by the bioaccumulation term in Eq. (4), than for Na and Mg (Table 6).
511 In relation to the mean W_{budget} , the combined uncertainty was of the same order of magnitude for Na, about the
512 half for Ca, one-third for K, and lower for Mg.

513

514 By using the weathering estimates obtained with PROFILE and the depletion method in the base cation budget
515 equation, Eq. (4), in combination with measured estimates of deposition, leaching and uptake in biomass,
516 alternative soil balances were estimated (Fig. 5). Since the base cation budget method predicted much higher
517 weathering rates than the other methods, a balance of sources and sinks consequently required more marked
518 decreases in exchangeable soil stocks for K, Ca and Mg when weathering rates were based on PROFILE or the
519 depletion method. Furthermore, as a consequence of the substantially higher W_{profile} for Na, the PROFILE based
520 base cation budget suggested substantial increases in exchangeable Na stocks.

521 4. Discussion

522 4.1 Comparison of conceptually different methods

523 A number of studies have used multiple approaches to estimate weathering rates, with the aim of validating
524 methods and finding a best estimate for a particular site or catchment (Langan et al., 1995; Kolka et al., 1996;
525 Sverdrup et al., 1998; Futter et al., 2012). A common problem encountered is that differences in quantities, are
526 not only complicated by conceptual differences between the approaches, but also by the fact that the comparisons
527 are not carried out in a harmonized way, i.e. at the same scale (pedon/catchment), using identical sampling
528 locations and methods for common input data, and consistent assumptions about the weathering zone (i.e. 0-50
529 cm or 0-100 cm). Concerning the spatial scale, the base cation approach has more commonly been applied at the
530 catchment and forest stand scale, whereas the depletion method and the PROFILE model are normally applied at
531 the pedon scale. In the present study, the base cation budget approach included data at stand level over a period
532 when the stand showed a high nutrient demand. Concerning the temporal scale, the concepts of the depletion
533 method and the PROFILE model are conceptually different, although they can be applied at similar spatial scale.
534 In the present study, these two methods are based on direct measurements of soil properties, i.e. quantitative
535 mineralogy, soil bulk density and soil stone content, which was rarely the case in previous comparable studies.
536 Since the three approaches used here do not measure similar quantities at spatial and temporal scale, and all of
537 them have obvious weaknesses, no estimate can be taken as the "true" weathering rate. However, the conceptual
538 differences between the three approaches are an asset, as they provide complementary information about
539 weathering at different scales that helps to identify strengths and weaknesses of each method and establish reasons
540 as to why these methods tend to vary in estimated weathering rates of particular elements.

541 4.2 Depletion method estimates versus PROFILE model estimates

542 Modelled (W_{profile}) and historical ($W_{\text{depletion}}$) base cation weathering rates were within the range of recently
543 published data for similar forest sites on podzolised glacial till (Stendahl et al., 2013). However, the historical
544 weathering rates at Asa were similar to the lowest historical weathering rate observed by Stendahl et al. (2013)
545 and the historical weathering rates for Flakaliden were similar to their highest rates, at least with regard to Ca and
546 Mg.

547

548 Our first test criterion was the overall weathering rate over 0-50 cm depth in the soil profile. A major finding was
549 that W_{profile} was higher than $W_{\text{depletion}}$ for Na and K. Similarly, high ratios of $W_{\text{profile}}/W_{\text{depletion}}$ of 4 were found at

550 catchment scale by Augustin et al. (2016). At the pedon scale, Stendahl et al. (2013) found $W_{\text{profile}}/W_{\text{depletion}}$ ratios
551 of on average 2.7 for 16 Swedish study sites (with average max. and min. ratios of 7.9 and 0.4, respectively); this
552 ratio was larger than the one found for Flakaliden in our study (1.5) and lower than the one found for Asa (5.1).
553 Similar to Flakaliden, low ratios have been reported for the Lake Gårdsjön site situated in south-western Sweden
554 (Sverdrup et al., 1998; Stendahl et al., 2013). An exception to the general trend of higher steady-state PROFILE
555 weathering rates compared to historical rates calculated by the depletion method, was found for Mg at the
556 Flakaliden site, where $W_{\text{depletion}}$ was 1.9-fold greater than W_{profile} in the upper mineral soil, but only at Flakaliden.
557 This exception with regard to Mg was also found by Stendahl et al. (2013) for all of their 16 study sites.

558

559 However, the estimated weathering rates are relevant for different temporal scales. Several studies have concluded
560 that the average historical weathering rate should generally be higher than the present weathering rate, since soil
561 development involves loss of easily weatherable minerals and ageing of mineral surfaces (Bain et al., 1993; Taylor
562 and Blum, 1995; White et al., 1996). In a study using the Historic-SAFE model, applied to the Lake Gårdsjön
563 catchment in southwestern Sweden, Sverdrup et al. (1998) predicted a decline in weathering rates due to assumed
564 disappearance of fine particles and loss of minerals. Their results suggested an increase in weathering rates from
565 deglaciation 12,000 years B.P. towards a peak at 9000 years B.P., followed by a gradual decrease to below initial
566 levels.

567

568 With this background, it may not seem surprising that our second test, postulating similarity between methods
569 concerning the weathering rate gradient with soil depth, was not fulfilled. We may imagine a front of intense
570 weathering moving downward through the soil profile over the millennia. Each horizon would undergo an episode,
571 limited in time, of intense weathering followed by slower weathering in the ageing material. The sensitivity test
572 performed with PROFILE revealed that the model output was only little affected by the differences in mineralogy
573 between horizons. Therefore, if processes are correctly modelled with PROFILE, the notion of a weathering front
574 should primarily be associated with changes in bulk density and exposed mineral surface area, as also suggested
575 by the positive correlation between W_{profile} and exposed mineral surface area and bulk density (Figs. S1-S2) and
576 by the findings of Jönsson et al. (1995).

577

578 The intense weathering at depth simulated by PROFILE is obviously in contrast with the classic notion of
579 weathering rates being highest in the A- or E-horizon of podzolised soils (Tamm, 1931). To test whether the high
580 W_{profile} values were possible to reconcile with the observed historical weathering, the hypothetical time needed for
581 the PROFILE weathering rates to accomplish the element losses determined with the depletion method was
582 calculated. The highest weathering rate, presently prevailing at approximately 80 cm (Asa) or 60 cm (Flakaliden)
583 depth according to PROFILE (Fig. 2), would cause the observed depletion losses within less than half of the soil
584 age ('max rates' in Fig. 6), potentially in concert with the concept of a weathering front. However, the calculation
585 also showed that the present minimum weathering rate, presently simulated for the topmost 1-3 layers (Fig. 2),
586 would often result in a more severe base cation depletion within less than the postglacial period than observed by
587 the depletion method ('min rates' in Fig. 6), particularly at Flakaliden, and for K and Na also at Asa. Provided

588 that the current weathering rate did not substantially exceed the historical average, this suggests a positive bias in
589 W_{profile} at the investigated sites.

590

591 The weathering rates of PROFILE may also be criticized based on discrepancies in the ranking order of weathering
592 of elements, compared to historical weathering; this is our third test criterion. PROFILE predicted the highest
593 steady-state weathering for Na at both sites. However, historical weathering at Asa was greatest for Ca among the
594 base cation elements, whereas Mg was the most abundant element released at Flakaliden. The latter was also
595 found by Olsson and Melkerud (2000), who reported the same ranking order of individual base cation weathering
596 (i.e. $\text{Mg} > \text{Ca} > \text{Na} > \text{K}$) for other sites in northern Sweden. At the mineralogical level, Casetou-Gustafson et al. (*this*
597 *issue*) demonstrates that K-feldspar was the dominant source of all steady state PROFILE weathering of K and
598 there are indications that the dissolution rate for K-feldspar is too high compared with mica. For example,
599 Thompson and Ukrainczyk (2002) described differences in the plant availability of K via weathering from these
600 two mineral groups. In addition, Simonsson et al. (2016) found that, although K-feldspar contained approximately
601 90% of the bulk K in the soil, 25-50% of the weathering of K had occurred in mica. Furthermore, and in more
602 general terms, Hodson and Langan (1999) suggested that the PROFILE model overestimates weathering rates
603 because it does not consider the decrease in mineral reactivity that has taken place over time and because it
604 assumes that all mineral surface areas are reactive. If this is not accounted for, PROFILE can be expected to
605 overestimate base cation weathering rates.

606

607 As to possible bias in the historical weathering rates, underestimates are possible at Asa, where the low values of
608 $W_{\text{depletion}}$ can be attributed to the low gradient of Zr in the soil (Fig. 5). This might, in turn, be the result of soil
609 mixing by different means. Mechanical soil scarification was carried out at both Asa and Flakaliden prior to
610 planting of the present stand, which would at least have caused partial mixing or inversion of surficial soil layers.
611 In addition, clearance cairns of unknown age were found in the experimental area at Asa, indicating small-scale
612 agriculture in the past. Moreover, if burrowing earthworms have been abundant in the past, they might have
613 produced soil mixing in the upper soil horizons (Taylor et al., 2019), resulting in a disturbed Zr gradient (Fig. 2)
614 and in low estimates of historical weathering in the rooting zone (Whitfield et al. 2011). High or near-neutral soil
615 pH and deciduous litter can promote high population densities of burrowing earthworms following forest clearing
616 and agriculture; partly deciduous vegetation dominated at Asa until only 1000-2000 years BP, with species such
617 as *Corylus avellana* (L.), *Betula* spp., *Quercus* spp. and *Tilia* spp. (Greisman et al., 2009).

618

619 Apart from disturbances, natural variability in weathering rates can likely be attributed to differences in soil
620 texture (i.e. exposed mineral surface area), climate (i.e. temperature and water percolation rate) and mineralogy.
621 At Flakaliden, it was reasoned that heterogeneous Zr gradients (Fig. 2) and Zr/base cation ratios (Fig. S3)
622 disqualified two soil profiles from further analysis, which would have otherwise indicated unreasonable net gains
623 of elements in the rooting zone (0-50 cm) (i.e. for soil profile 15A for all elements and for soil profile 11B with
624 regard to Na and K). Whitfield et al. (2011) used the same argument for excluding single profiles from their
625 calculations, emphasizing that overall gains in the rooting zone are not expected without external additions of
626 base cations to the soil profiles. Several alternative reasons could have contributed to the observed peaks of Zr in

627 the B/C-horizon at Flakaliden, such as local heterogeneities of the deposited till, which was suggested by the
628 unstable Ti/Zr ratio in soil profile 15A and 11B. However, the observed peaks in the Ti/Zr gradients were only
629 explained by irregularities in Ti gradients (i.e. increases in the Ti/Zr ratio indicate that Ti concentrations are
630 increasing) the latter has to be treated carefully since in cases where both Zr and Ti show inconsistent patterns
631 with soil depth, the Ti/Zr ratio will still be stable and hereby overshadows heterogeneities observed with soil depth
632 for both elements (Fig. 1, 2). Thus, heterogeneities in Zr gradients observed in the B/C horizon can be attributed
633 to local heterogeneities of the parent material irrespective of if the Ti/Zr gradients are stable at these depths.

634

635 Regardless of errors in the Zr gradients, both $W_{\text{depletion}}$ and W_{profile} showed more marked gradients with soil depth
636 at Flakaliden compared to Asa. This could be expected based on the more well-developed podzol profile at
637 Flakaliden. It has been postulated that the formation of podzols is enhanced by long duration and great depth of
638 snow cover (Jauhiainen, 1973; Schaetzl and Isard, 1996), which would imply that soil formation had progressed
639 further at Flakaliden than at Asa (Lundström et al., 2000). At Flakaliden, the average mass loss of Ca and Mg was
640 4.0-fold larger in the E-horizon than in the B-horizon, which is similar to findings by Olsson and Melkerud (2000)
641 of a 5-fold higher ratio between losses of base cations in the E- compared with the B-horizon.

642 **4.3 Weathering in a base cation budget perspective**

643 The base cation budget approach consistently resulted in much higher weathering rates than PROFILE and the
644 depletion method for all base cations except Na. However, as was shown by the large combined uncertainties
645 given in Table 6, base cation budget estimates of weathering are associated with substantial uncertainties from
646 different sources. Similar large uncertainties associated with estimates of W_{budget} were observed by Simonsson et
647 al. (2015) for the Skogaby site in south-western Sweden, a Norway spruce site of similar stand age and soil
648 condition as Asa.. Accounting for all sources of uncertainty, they found that the 95% confidence interval in
649 estimates of base cation weathering was 2.6 times the mean (33 $\text{mmol}_c \text{ m}^{-2} \text{ yr}^{-1}$).

650 Despite the considerable uncertainties in W_{budget} estimates, the base cation budget approach illustrated that
651 accumulation in biomass was a dominant sink for all base cation elements except Na. This is in line with findings
652 by Nykvist (2000) for two Norway spruce sites in Sweden and the study by Simonsson et al. (2015). However, it
653 contrasts to conditions in other studies of no change in soil and tree biomass stocks of base cations (e.g. Sverdrup
654 et al., 1998). The higher estimates of weathering rate at Asa reflected the higher productivity and nutrient demand
655 of the stand at this site (Bergh et al., 1999), which has resulted in 1.4-fold greater accumulation of base cations in
656 biomass than at Flakaliden.

657 The Na fluxes differed from those of the other base cations, probably because Ca, Mg and K are important plant
658 nutrients whereas Na is not. Calcium and Mg uptake in forest trees is considered to be more or less passive flow
659 driven by transpiration fluxes, whereas K uptake is an energy-demanding active process (Nieves-Cordones et al.,
660 2014). Considering that Na was the dominant base cation in the soil solution at 50 cm soil depth (Fig. 5), the
661 negligible accumulation of Na in tree biomass suggests that Na uptake in trees is physiologically blocked. Low
662 concentrations of Na seem to be a general feature of terrestrial plants in boreal forests, in contrast to aquatic plants,

663 which explains why the latter are considered important Na sources for large herbivores like moose (Ohlson and
664 Staaland, 2001). Thus, the negligible Na accumulation in tree biomass and the particularly low deposition at
665 Flakaliden simplify the Na budget to only three major counterbalancing fluxes: weathering, deposition and
666 leaching. Since $W_{\text{depletion}}$ and W_{budget} of Na were fairly similar, and were much lower than W_{profile} , our results provide
667 additional support for the claim that the PROFILE model produced consistently too high Na weathering.

668 Accumulation of Ca, Mg and K in biomass made up the dominant sink. Since deposition and measured depletion
669 of extractable Ca, K and Mg in the soil did not balance this sink, substantial missing sources, here estimated as
670 an apparent weathering rate, were needed to reach a balance. Using the alternative weathering estimates by
671 PROFILE and the depletion method in the base cation budget resulted in even larger estimated depletion in the
672 soil to balance the sinks than was actually measured. Uncertainties in estimating soil changes were probably
673 significant, since the estimates of soil depletion were based on two single measurements over 12 years and the
674 extraction procedures were not identical over time. Nevertheless, the changes observed in extractable Ca stocks
675 in the soil are in line with observations over 22 years of aggrading Norway spruce forests by Zetterberg et al.
676 (2016), who reported exchangeable Ca depletion rates of 5-11 and 23-39 $\text{mmol}_c \text{ m}^{-2} \text{ yr}^{-1}$ for sites in south-western
677 and northern Sweden, respectively. The higher value for the northern site reflected higher Ca saturation in the
678 soil. The corresponding values for Asa and Flakaliden were larger, but of similar magnitude (34.5 and 40.5 mmol_c
679 $\text{m}^{-2} \text{ yr}^{-1}$, respectively). Brandtberg and Olsson (2012) studied the same sites as Zetterberg et al. (2016) over a 10-
680 year period and found a general minor increase in extractable K soil stocks and a substantial decrease in the Ca
681 stocks, a result much similar to the findings of the present study. The results therefore suggest that other sources
682 of nutrient base cations exist in the soil, apart from weathering ($W_{\text{depletion}}$, W_{profile}) and depletion of ammonium-
683 chloride-extractable base cation stocks. Regarding K, fixed or structural K in clay minerals provides a dynamic
684 pool of K that is not included in modelled weathering or in NH_4Cl -extractable K (Simonsson et al., 2016).
685 Regarding Ca and Mg, dissolution from non-crystalline/amorphous compounds can be an important source in
686 soils depleted of these elements (Van der Heijden et al., 2017).

687 There are other possible explanations for the higher weathering rates with the base cation budget approach
688 compared to PROFILE for K, Mg and Ca. First, it is possible that the assumption made that no base cation uptake
689 takes place below 50 cm in the soil was wrong. If trees can take up base cations from deeper soil horizons (e.g.
690 Brantley et al., 2017), the discrepancy in weathering rates between the two methods would be reduced since
691 PROFILE predicted higher weathering rates with increasing depth. Second, PROFILE may produce conservative
692 estimates of present-day weathering because the model only captures steady-state chemical processes. It has been
693 postulated that e.g. mycorrhizae play an important role in nutrient uptake in forest trees through active foraging
694 by mycelia at mineral surfaces, but the nature and quantitative importance of biotic control or stimulation of
695 weathering has been much debated in recent decades (Finlay et al., 2009; Sverdrup, 2009; Smits and Wallander,
696 2017; Finlay et al., *this issue*). Thus, the results from the present study do not contradict the view that such
697 processes can be quantitatively important in field situations.

698 **5. Conclusions**

699 The release rate of important plant nutrients from the mineral soil has been previously shown to differ largely
700 when estimated with different methods due to a lack of uniformity in method comparison and data collection,
701 which has made it impossible to understand conceptual similarities and dissimilarities between methods. Three
702 conceptually different methods were compared in a harmonized fashion for 8 soil profiles at two long-term
703 experimental forest sites with the aim of quantifying variability in weathering rate estimates and making concrete
704 suggestions for an improved future applicability of these methods.

705

706 The results indicated that historical weathering estimated by the depletion method was probably underestimated,
707 particularly at Asa, or was reasonably accurate (Ca, Mg). Reasons for underestimated weathering rates at Asa was
708 that all criteria for application of the method were not well fulfilled. The weakly developed and possibly erratic
709 Zr gradients in the soil at Asa could have been caused by natural and anthropogenic disturbances. Future studies
710 based on the depletion method should ensure that the Zr gradient with depth show a net enrichment of Zr towards
711 the soil surface. This condition was not fulfilled for soil profiles at the Asa site. Another important outcome of
712 the study was to show that within-site variations in Zr gradients can be large, as was the case at Flakaliden. At
713 that site, two soil profiles showed obviously erratic Zr gradients for unknown reasons and were not included in
714 estimates of site mean weathering rates. In sharp contrast to the depletion method, steady-state weathering by
715 PROFILE increased with increasing soil depth, and weathering rates were also generally higher. PROFILE
716 probably produced reasonably accurate estimates of present-day weathering rates, rather than underestimates, but
717 likely overestimated weathering of Na and K. This conclusion was based on differences between historical and
718 steady-state estimates in rank-order of elements, and that the back-calculation of current PROFILE weathering
719 rates to simulate historic base cation losses suggested a rapid depletion of Na and K even at the lowest PROFILE
720 weathering rates. A possible reason that K weathering rates were also overestimated by the PROFILE method
721 were inappropriate dissolution rates for K-bearing minerals applied in the model, which should be accounted for
722 in future PROFILE based weathering estimate.

723

724 In the second comparison including three methods, the base cation budget method produced much higher
725 estimates of present-day weathering compared to estimates by the other methods, except for Na. This discrepancy
726 was largely an effect of the large uptake rates of Ca, K and Mg in the biomass, in contrast to negligible
727 accumulation of Na, and that this uptake was only partly balanced by measured depletion of extractable soil pools,
728 particularly for Ca. The large discrepancy in weathering rates between the base cation budget method and the
729 other methods suggest that there were additional sources available for uptake particularly of Ca and K by trees
730 in the soil besides weathering and the measured depletion in extractable base cations.

731

732 **6. Authors contribution**

733 Authors contributed to the study as in the following: S. Casetou-Gustafson: study design, data treatment, analyses,
734 interpretation and writing. Magnus Simonsson: study design, analysis, interpretation and writing. Johan Stendahl:
735 study design, analysis, interpretation and writing B.A. Olsson: study design, data treatment, analysis,

736 interpretation and writing. S. Hillier: interpretation and writing. Sune Linder: Provided long-term experimental
737 data, interpretation and writing. Harald Grip: Provided long-term experimental data, interpretation, and writing

738 **7. Acknowledgements**

739 Financial support from The Swedish research Council for Environment, Agricultural Sciences and Spatial Planning
740 (212-2011-1691) (FORMAS) (Strong Research Environment, QWARTS) and the Swedish Energy Agency
741 (p36151-1). Stephen Hillier acknowledges support of the Scottish Government's Rural and Environment Science
742 and Analytical Services Division (RESAS). We thank Cecilia Akselsson for her contribution to study design,
743 PROFILE model development and valuable comments on earlier versions of the manuscript.

744

745 **8. References**

746 Akselsson, C., Westling, O., Sverdrup, H., Holmqvist, J., Thelin, G., Uggla, E., and Malm, G.: Impact of harvest
747 intensity on long-term base cation budgets in Swedish forest soils, *Water Air Soil Poll.: Focus*, 7, 201-210, 2007.

748 Akselsson, C., Belyazid, S., Stendahl, J., Finlay, R., Olsson, B.A., Erlandsson Lampa, M., Wallander, H.,
749 Gustafsson, J.P., and Bishop, K. H.: Weathering rates in Swedish forest soils, In review in *Biogeosciences* (this
750 issue).

751 Albaugh, T. J., Bergh, J., Lundmark, T., Nilsson, U., Stape, J. L., Allen, H. L., and Linder, S.: Do biological
752 expansion factors adequately estimate stand-scale aboveground component biomass for Norway spruce?, *Forest*
753 *Ecol. Manag.*, 258, 2628-2637, 2009.

754 Albaugh, T. J., Bergh, J., Lundmark, T., Nilsson, U., Stape, J. L., Allen, H. L., and Linder, S.: Corrigendum to
755 “Do biological expansion factors adequately estimate stand-scale aboveground component biomass for Norway
756 spruce?”, *Forest Ecol. Manag.*, 270, 314, 2012.

757 Augustin, F., Houle, D., Gagnon, C., and Courchesne, F.: Evaluation of three methods for estimating the
758 weathering rates of base cations in forested catchments, *Catena*, 144, 1-10, 2016.

759 Bailey, S. W., Buso, D. C., and Likens, G. E.: Implications of sodium mass balance for interpreting the calcium
760 cycle of a forested ecosystem, *Ecology*, 84, 471-484, 2003.

761 Bain, D. C., Mellor, A., Robertson-Rintoul, M., and Buckland, S.: Variations in weathering processes and rates
762 with time in a chronosequence of soils from Glen Feshie, Scotland, *Geoderma*, 57, 275-293, 1993.

763 Bain, D. C., Mellor, A., Wilson, M., and Duthie, D.: Chemical and mineralogical weathering rates and processes
764 in an upland granitic till catchment in Scotland, *Water Air Soil Poll.*, 73, 11-27, 1994.

765 Bergh, J., Linder, S., Lundmark, T., and Elfving, B.: The effect of water and nutrient availability on the
766 productivity of Norway spruce in northern and southern Sweden, *Forest Ecol. Manag.*, 119, 51-62, 1999.

767 Bergh, J., Linder, S., and Bergström, J.: Potential production of Norway spruce in Sweden, *Forest Ecol. Manag.*,
768 204, 1-10, 2005.

769 Brandtberg, P.-O., Olsson, B.A.: Changes in the effects of whole-tree harvesting on soil chemistry during 10
770 years of stand development. *For. Ecol. and Manage.*, 277, 150-162, 2012.

771 Brantley, S.L., Eissenstat, D.M., Marshall, J.A., Godsey, S.E., Balogh-Brunstad, Z., Karwan, D.L., Papuga,
772 S.A., Roering, J., Dawson, T.E., Evaristo, J. (2017) Reviews and syntheses: on the roles trees play in building
773 and plumbing the critical zone. *Biogeosciences* (Online) 14.

774 Brimhall, G. H., Ford, C., Bratt, J., Taylor, G., and Warin, O.: Quantitative geochemical approach to pedogenesis:
775 importance of parent material reduction, volumetric expansion, and eolian influx in lateritization, *Geoderma*, 51,
776 51-91, 1991.

777 Casetou-Gustafson, S., Hillier, S., Akselsson, C., Simonsson, M., Stendahl, J., and Olsson, B. A.: Comparison of
778 measured (XRPD) and modeled (A2M) soil mineralogies: A study of some Swedish forest soils in the context of
779 weathering rate predictions, *Geoderma*, 310, 77-88, 2018.

780 Casetou-Gustafson, S., Akselsson, C., Hillier, S., and Olsson, B. A.: The importance of mineral composition
781 determinations to PROFILE base cation release rates: A case study, *Biogeosciences* (this issue), 1903–1920, 2019.

782 Chadwick, O. A., Brimhall, G. H., and Hendricks, D. M.: From a black to a gray box—a mass balance
783 interpretation of pedogenesis, *Geomorphology*, 3, 369-390, 1990.

784 Cosby, B., Hornberger, G., Galloway, J., and Wright, R.: Modeling the effects of acid deposition: Assessment of
785 a lumped parameter model of soil water and streamwater chemistry, *Water Resour. Res.*, 21, 51-63, 1985.

786 Erlandsson Lampa, M., Sverdrup, H.U., Bishop, K.H., Belyazid, S., Ameli, A., and Köhler, S. J.: Catchment
787 export of base cations: Improved mineral dissolution kinetics influence the role of water transit time, In review in
788 *Biogeosciences* (this issue).

789 Finlay, R., Wallander, H., Smits, M., Holmström, S., Van Hees, P., Lian, B., and Rosling, A.: The role of fungi
790 in biogenic weathering in boreal forest soils, *Fungal Biol. Rev.*, 23, 101-106, 2009.

791 Finlay, R.D., Mahmood, S., Rosenstock, N., Bolou-bi, E., Köhler, S.J., Fahad, Y., Rosling, Wallander, H.,
792 Belyazid, S., Bishop, K., Lian, B. Biological weathering and its cosequence at different spatial levels – from
793 nanosclae to global sclae. *Biogeosciences*. In review in *Biogeosciences* (this issue).

794 Fredén, C.: *The National Atlas of Sweden, Geology, Third Ed.* SNA Publishing House, Stockholm, Sweden, 2009.

795 Fröberg, M., Berggren, D., Bergkvist, B., Bryant, C., & Mulder, J. (2006). Concentration and Fluxes of Dissolved
796 Organic Carbon (DOC) in Three Norway Spruce Stands along a Climatic Gradient in
797 Sweden. *Biogeochemistry*, 77(1), 1-23.

798 Fröberg, M., Grip, H., Tipping, E., Svensson, M., Strömngren, M., and Kleja, D. B.: Long-term effects of
799 experimental fertilization and soil warming on dissolved organic matter leaching from a spruce forest in Northern
800 Sweden, *Geoderma*, 200, 172-179, 2013.

801 Futter, M., Klaminder, J., Lucas, R., Laudon, H., and Köhler, S.: Uncertainty in silicate mineral weathering rate
802 estimates: source partitioning and policy implications, *Environ Res. Lett.*, 7, 024025, 2012.

803 Greisman, A., and Gaillard, M. J.: The role of climate variability and fire in early and mid Holocene forest
804 dynamics of southern Sweden, *J. Quaternary Sci.*, 24, 593-611, 2009.

805 Grennfelt, P., and Hov, Ø.: Regional air pollution at a turning point, *Ambio*, 2-10, 2005.

806 Harden, J. W.: Soils developed in granitic alluvium near Merced, California, *Geological Survey Bulletin (USA)*
807 1590-A, *Soil Chronosequences in the Western United States*, Government Printing Office, Washington DC, USA,
808 A1–A65, 1987.

809 Hedin, L. O., Granat, L., Likens, G. E., Buishand, T. A., Galloway, J. N., Butler, T. J., and Rodhe, H.: Steep
810 declines in atmospheric base cations in regions of Europe and North America, *Nature*, 367, 351-354, 1994.

811 Hedwall, P. O., Grip, H., Linder, S., Lövdahl, L., Nilsson, U., and Bergh, J.: Effects of clear-cutting and slash
812 removal on soil water chemistry and forest-floor vegetation in a nutrient optimised Norway spruce stand, *Silva*
813 *Fenn.*, 47, article id 933, 2013.

- 814 Hellsten, S., Helmisaari, H. S., Melin, Y., Skovsgaard, J. P., Kaakinen, S., Kukkola, M., Saarsalmi, A., Petersson,
815 H., and Akselsson, C.: Nutrient concentrations in stumps and coarse roots of Norway spruce, Scots pine and silver
816 birch in Sweden, Finland and Denmark, *Forest Ecol. Manag.*, 290, 40-48, 2013.
- 817 Helmisaari, H.-S., Derome, J., Nöjd, P., and Kukkola, M.: Fine root biomass in relation to site and stand
818 characteristics in Norway spruce and Scots pine stands, *Tree Physiol.*, 27, 1493-1504, 2007.
- 819 Hillier, S.: Use of an air brush to spray dry samples for X-ray powder diffraction, *Clay Miner.*, 34, 127-127, 1999.
- 820 Hillier, S.: Quantitative analysis of clay and other minerals in sandstones by X-ray powder diffraction (XRPD),
821 in: *Clay Mineral Cements in Sandstones*, edited by: Worden, R., Morad, S.: International Association of
822 Sedimentologist, Special Publication, John Wiley and Sons Ltd, Oxford, United Kingdom, 34, 213-251, 2003.
- 823 Hodson, M. E., Langan, S. J., and Wilson, M. J.: A sensitivity analysis of the PROFILE model in relation to the
824 calculation of soil weathering rates, *Appl. Geochem.*, 11, 835-844, 1996.
- 825 Hodson, M. E., and Langan, S. J.: The influence of soil age on calculated mineral weathering rates, *Appl.*
826 *Geochem.*, 14, 387-394, 1999.
- 827 Jansson, P.-E.: CoupModel: model use, calibration, and validation, *Trans. Am. Soc. Agric. Eng.*, 55, 1337-1344,
828 2012.
- 829 Jauhiainen, E.: Age and degree of podzolization of sand soils on the coastal plain of northwest Finland, *Comm.*
830 *Biol.*, 68, 1-32, 1973.
- 831 Jönsson, C., Warfvinge, P., and Sverdrup, H.: Uncertainty in predicting weathering rate and environmental stress
832 factors with the PROFILE model, *Water Air Soil Poll.*, 81, 1-23, 1995.
- 833 Karlsson, P. E., Ferm, M., Hultberg, H., Hellsten, S., Akselsson, C., and Pihl Karlsson, G.: Totaldeposition av
834 kväve till skog, IVL Swedish Environmental Research Institute, Stockholm, Sweden 37, 2012.
- 835 Karlsson, P. E., Ferm, M., Hultberg, H., Hellsten, S., Akselsson, C., and Pihl Karlsson, G.: Totaldeposition av
836 baskatjoner till skog, IVL Swedish Environmental Research Institute, Stockholm, Sweden 65, 2013.
- 837 Kellner, O.: Effects of fertilization on forest flora and vegetation, Ph.D. thesis, *Comprehensive Summaries of*
838 *Uppsala Dissertations from the Faculty of Science*, Uppsala University, Sweden, 464, 32 pp., 1993.
- 839 Klaminder, J., Lucas, R., Futter, M., Bishop, K., Köhler, S., Egnell, G., and Laudon, H.: Silicate mineral
840 weathering rate estimates: Are they precise enough to be useful when predicting the recovery of nutrient pools
841 after harvesting?, *Forest Ecol. Manag.*, 261, 1-9, 2011.
- 842 Kolka, R. K., Grigal, D., and Nater, E.: Forest soil mineral weathering rates: use of multiple approaches,
843 *Geoderma*. Vol. 73 (1): 1-21.(1996), 73, 1996.
- 844 Langan, S. J., Sverdrup, H. U., and Coull, M.: The calculation of base cation release from the chemical weathering
845 of Scottish soils using the PROFILE model, *Water Air Soil Poll.*, 85, 2497-2502, 1995.
- 846 Likens, G. E., and Bormann, F. H.: Acid rain: a serious regional environmental problem, *Science*, 184, 1176-
847 1179, 1974.
- 848 Likens, G. E., Driscoll, C. T., Buso, D. C., Siccama, T. G., Johnson, C. E., Lovett, G. M., Fahey, T. J., Reiners,
849 W. A., Ryan, D. F., Martin, C. W., and Bailey, S. W.: The biogeochemistry of calcium at Hubbard Brook,
850 *Biogeochemistry*, 41, 89-173, 1998.
- 851 Linder, S.: Foliar analysis for detecting and correcting nutrient imbalances in Norway spruce, *Ecol. Bull.*
852 (Copenhagen), 178-190, 1995.
- 853 Lundström, U., Van Breemen, N., Bain, D., Van Hees, P., Giesler, R., Gustafsson, J. P., Ilvesniemi, H., Karlton,
854 E., Melkerud, P.-A., and Olsson, M.: Advances in understanding the podzolization process resulting from a
855 multidisciplinary study of three coniferous forest soils in the Nordic Countries, *Geoderma*, 94, 335-353, 2000.

- 856 Löfgren, S., Aastrup, M., Bringmark, L., Hultberg, H., Lewin-Pihlblad, L., Lundin, L., Karlsson, G. P., and
857 Thunholm, B.: Recovery of soil water, groundwater, and streamwater from acidification at the Swedish Integrated
858 Monitoring catchments, *Ambio*, 40, 836-856, 2011.
- 859 Marklund, L. G.: Biomass functions for pine, spruce and birch in Sweden, Department of Forest Survey, Swedish
860 University of Agricultural Sciences, Umea, Sweden, Report 45, 1–73, 1988.
- 861 Marshall, C., and Haseman, J.: The quantitative evaluation of soil formation and development by heavy mineral
862 studies: A Grundy silt loam profile 1, *Soil Sci. Soc. Am. J.*, 7, 448-453, 1943.
- 863 Nieves-Cordones, M., Alemán, F., Martínez, V., and Rubio, F.: K⁺ uptake in plant roots. The systems involved,
864 their regulation and parallels in other organisms, *Journal of plant physiology*, 171, 688-695, 2014.
- 865 Nilsson, S. I., Miller, H. G., and Miller, J. D.: Forest growth as a possible cause of soil and water acidification -
866 an examination of the concepts, *Oikos*, 39, 40-49, 1982.
- 867 Nykvist, N.: Effects of clearfelling, slash removal and prescribed burning on amounts of plant nutrients in biomass
868 and soil, Swedish University of Agricultural Sciences, Department of Forest Ecology, Uppsala, Sweden, 210,
869 2000.
- 870 Ohlson, M., and Staaland, H.: Mineral diversity in wild plants: benefits and bane for moose, *Oikos*, 94, 442-454,
871 2001.
- 872 Olsson, B. A., Bengtsson, J., and Lundkvist, H.: Effects of different forest harvest intensities on the pools of
873 exchangeable cations in coniferous forest soils, *Forest Ecol. Manag.*, 84, 135-147, 1996.
- 874 Olsson, M., and Melkerud, P.-A.: Chemical and mineralogical changes during genesis of a Podzol from till in
875 southern Sweden, *Geoderma*, 45, 267-287, 1989.
- 876 Olsson, M. T., and Melkerud, P.-A.: Weathering in three podzolized pedons on glacial deposits in northern
877 Sweden and central Finland, *Geoderma*, 94, 149-161, 2000.
- 878 Olsson, M., Rosén, K., and Melkerud, P.-A.: Regional modelling of base cation losses from Swedish forest soils
879 due to whole-tree harvesting, *Appl Geochem*, 8, 189-194, 1993.
- 880 Omotoso, O., McCarty, D. K., Hillier, S., and Kleeberg, R.: Some successful approaches to quantitative mineral
881 analysis as revealed by the 3rd Reynolds Cup contest, *Clay Clay Miner.*, 54, 748-760, 2006.
- 882 Petersson, H., and Ståhl, G.: Functions for below-ground biomass of *Pinus sylvestris*, *Picea abies*, *Betula pendula*
883 and *Betula pubescens* in Sweden, *Scand. J. Forest Res.*, 21, 84-93, 2006.
- 884 Reuss, J. O., and Johnson, D.W.: Acid Deposition and the Acidification of Soils and Waters, *Ecol. Stud.*, 95,
885 1986.
- 886 Ryan, M. G.: Three decades of research at Flakaliden advancing whole-tree physiology, forest ecosystem and
887 global change research, *Tree Physiol.*, 33, 1123-1131, 2013.
- 888 Schaetzl, R. J., and Isard, S. A.: Regional-scale relationships between climate and strength of podzolization in the
889 Great Lakes region, North America, *Catena*, 28, 47-69, 1996.
- 890 Schützel, H., Kutschke, D., and Wildner, G.: Zur Problematik der Genese der Grauen Gneise des sächsischen
891 Erzgebirges (zirkonstatistische Untersuchungen), VEB Deutscher Verlag für Grundstoffindustrie, Leipzig, 1963.
- 892 Sigurdsson, B. D., Medhurst, J. L., Wallin, G., Eggertsson, O., and Linder, S.: Growth of mature boreal Norway
893 spruce was not affected by elevated [CO₂] and/or air temperature unless nutrient availability was improved, *Tree*
894 *Physiol.*, 33, 1192-1205, 2013.
- 895 Simonsson, M., and Berggren, D.: Aluminium solubility related to secondary solid phases in upper B horizons
896 with spodic characteristics, *Eur. J. Soil Sci.*, 49, 317-326, 1998.

897 Simonsson, M., Bergholm, J., Olsson, B. A., von Brömssen, C., and Öborn, I.: Estimating weathering rates using
898 base cation budgets in a Norway spruce stand on podzolised soil: analysis of fluxes and uncertainties, *Forest Ecol.*
899 *Manag.*, 340, 135-152, 2015.

900 Simonsson, M., Bergholm, J., Lemarchand, D., and Hillier, S.: Mineralogy and biogeochemistry of potassium in
901 the Skogaby experimental forest, southwest Sweden: pools, fluxes and K/Rb ratios in soil and biomass,
902 *Biogeochemistry*, 131, 77-102, 2016.

903 Smits, M. M., and Wallander, H.: Role of mycorrhizal symbiosis in mineral weathering and nutrient mining from
904 soil parent material, in: *Mycorrhizal Mediation of Soil: Fertility, Structure, and Carbon Storage*, edited by:
905 Johnson, N. C., Gehring, C., and Jansa, J., Elsevier, United States, 35-46, 2017.

906 Starr, M., Lindroos, A.-J., and Ukonmaanaho, L.: Weathering release rates of base cations from soils within a
907 boreal forested catchment: variation and comparison to deposition, litterfall and leaching fluxes, *Environ. Earth*
908 *Sci.*, 72, 5101-5111, 2014.

909 Stendahl, J., Lundin, L., and Nilsson, T.: The stone and boulder content of Swedish forest soils, *Catena*, 77, 285-
910 291, 2009.

911 Stendahl, J., Akselsson, C., Melkerud, P.-A., and Belyazid, S.: Pedon-scale silicate weathering: comparison of the
912 PROFILE model and the depletion method at 16 forest sites in Sweden, *Geoderma*, 211, 65-74, 2013.

913 Strengbom, J., Dahlberg, A., Larsson, A., Lindelow, A., Sandström, J., Widenfalk, O., and Gustafsson, L.:
914 Introducing intensively managed spruce plantations in Swedish forest landscapes will impair biodiversity decline,
915 *Forests*, 2, 610-630, 2011.

916 Sudom, M., and St. Arnaud, R.: Use of quartz, zirconium and titanium as indices in pedological studies, *Can. J.*
917 *Soil Sci.*, 51, 385-396, 1971.

918 Sverdrup, H.: Chemical weathering of soil minerals and the role of biological processes, *Fungal Biol. Rev.*, 23,
919 94-100, 2009.

920 Sverdrup, H., and Rosen, K.: Long-term base cation mass balances for Swedish forests and the concept of
921 sustainability, *Forest Ecol. Manag.*, 110, 221-236, 1998.

922 Sverdrup, H., and Warfvinge, P.: Weathering of primary silicate minerals in the natural soil environment in
923 relation to a chemical weathering model, *Water Air Soil Poll.*, 38, 387-408, 1988.

924 Sverdrup, H., Warfvinge, P., and Wickman, T.: Estimating the weathering rate at Gårdsjön using different
925 methods, in: *Experimental Reversal of Rain Effects: Gardsjon Roof Project*, edited by: Hultberg, H., and
926 Skeffington, R., John Wiley & Sons Ltd, Chichester, United Kingdom, 231-249, 1998.

927 Tamm, C.-O.: Nitrogen in Terrestrial Ecosystems: Questions of Productivity, Vegetational Changes, and
928 Ecosystem Stability. *Ecological Studies* 81, Springer-Verlag, Berlin, 115 p., 1991.

929 Tamm, O.: Studier över jordmånstyper och deras förhållande till markens hydrologi i nordsvenska skogsterräng
930 barrskogsområdet, *Reports of the Swedish Institute of Experimental Forestry*, 26(2), 163-355, 1931. (In Swedish)

931 Taylor, A., and Blum, J. D.: Relation between soil age and silicate weathering rates determined from the chemical
932 evolution of a glacial chronosequence, *Geology*, 23, 979-982, 1995.

933 Taylor, A., Lenoir, L., Vegerfors, B., and Persson, T.: Ant and earthworm bioturbation in cold-temperate
934 ecosystems, *Ecosystems*, 1-14, 2019.

935 Thompson, M. L., and Ukrainczyk, L.: Micas, Soil mineralogy with environmental applications, in: *Soil*
936 *Mineralogy with Environmental Applications*, edited by: Dixon, J. B., and Schulze, D. G., Soil Science Society
937 of America Inc., Madison, 431-466 pp., 2002.

938 Van Der Heijden, G., Legout, A., Mareschal, L., Ranger, J., and Dambrine, E.: Filling the gap in Ca input-output
939 budgets in base-poor forest ecosystems: The contribution of non-crystalline phases evidenced by stable isotopic
940 dilution, *Geochim. Cosmochim. Acta*, 209, 135-148, 2017.

941 Van der Salm, C.: Assessment of the regional variation in weathering rates of loess and clay soils in the
942 Netherlands, *Water Air Soil Poll.*, 131, 217-243, 2001.

943 Velbel, M. A.: Geochemical mass balances and weathering rates in forested watersheds of the southern Blue
944 Ridge, *Am. J. Sci.*, 285, 904-930, 1985.

945 Viro, P.: Kivisyyden maarittamisesta, Summary: On the determination of stoniness. *Commun. Inst. For. Fenn.*,
946 40, 8, 1952.

947 Warfvinge, P., and Sverdrup, H.: Critical Loads of Acidity to Swedish Forest Soils: Methods, Data and Results,
948 Reports in Ecology and Environmental Engineering, Dpt. of Chemical Engineering II, Lund University, Lund,
949 Sweden, 1995.

950 White, A. F., Blum, A. E., Schulz, M. S., Bullen, T. D., Harden, J. W., and Peterson, M. L.: Chemical weathering
951 rates of a soil chronosequence on granitic alluvium: I. Quantification of mineralogical and surface area changes
952 and calculation of primary silicate reaction rates, *Geochim. Cosmochim. Acta*, 60, 2533-2550, 1996.

953 Whitfield, C., Watmough, S., Aherne, J., Dillon, P.: A comparison of weathering rates for acid-sensitive
954 catchments in Nova Scotia, Canada and their impact on critical load calculations, *Geoderma* 136, 899-911, 2006.

955 Whitfield, C. J., Watmough, S. A., and Aherne, J.: Evaluation of elemental depletion weathering rate estimation
956 methods on acid-sensitive soils of north-eastern Alberta, Canada, *Geoderma*, 166, 189-197, 2011.

957 Wikström, P., Edenius, L., Elfving, B., Eriksson, L. O., Lämås, T., Sonesson, J., Öhman, K., Wallerman, J.,
958 Waller, C., and Klintebäck, F.: The Heureka forestry decision support system: an overview, *Mathematical and
959 Computational Forestry & Natural Resource Sciences*, 3, 87, 2011.

960 Zetterberg, T., Olsson, B. A., Löfgren, S., von Brömssen, C., and Brandtberg, P. O.: The effect of harvest intensity
961 on long-term calcium dynamics in soil and soil solution at three coniferous sites in Sweden, *Forest Ecol. Manag.*,
962 302, 280-294, 2013.

963 Zetterberg, T., Olsson, B. A., Löfgren, S., Hyvönen, R., and Brandtberg, P. O.: Long-term soil calcium depletion
964 after conventional and whole-tree harvest, *Forest Ecol. Manag.*, 369, 102-115, 2016.

965

966

967

Table 1. Soil profile characteristics at 50 cm depth in the mineral soil at the Asa and Flakaliden sites

Site	Plot	Clay (% wt)	Silt (% wt)	Sand (% wt)	Coarse (% wt)	Density (g/cm ³)	Soil age (calendar years)
Asa	K1	9.49	25.04	45.30	20.18	1.10	14300
	K4	7.65	22.59	39.21	30.48	1.09	14300
	F3	4.95	25.26	40.54	29.25	0.99	14300
	F4	8.64	25.69	40.13	25.54	0.94	14300
Flakaliden	15A	1.92	9.21	68.98	19.68	1.89	10150
	14B	7.71	34.09	33.71	24.17	1.35	10150
	10B	7.75	45.17	37.23	8.90	1.36	10150
	11B	9.56	45.07	33.91	10.72	1.47	10150

968

969

970 **Table 2.** A short description of characteristics of the three different approaches that are used in the study to
 971 estimate base cation release rates at the pedon scale using a harmonized set of input data. The difference between
 972 methods reflect expected differences due to different time scales, conceptual differences, assumptions about
 973 weathering kinetics and pedogenesis.

Description	PROFILE	Depletion	Base cation budget
Time scale	Present-day	Long-term	Present-day
Concept	Steady-state	Historical	Dynamic
Weathering kinetics	Long-term kinetics	No assumption	No assumption
Pedogenesis	No assumption	Zr immobility, unweathered and homogeneous parent material	No assumption

974

975

976

977

978

Table 3. Extractable concentrations of different elements at the reference depths used for calculating historical weathering rate at the Asa and Flakaliden sites.

Site	Plot	Ref. depth (cm)	Ca (%)	Mg(%)	K(%)	Na (%)	Zr (ppm)	Ti (%)
Asa	K1	80-90	1.41	0.51	0.93	1.06		0.34
	K4	80-90	1.29	0.44	0.88	1.00	288.1	-
	F3	60-70	1.41	0.55	0.87	1.04	282.6	-
	F4	80-90	1.26	0.49	0.85	0.98	293.3	-
Flakaliden	10B	60-70	1.09	0.57	0.88	0.87	243.8	-
	14B	60-70	1.59	0.70	0.81	1.03	336.1	-

979

980

981

982

983

984

Table 4a. Site parameters used in the PROFILE model

Parameter	Source	Asa	Flakaliden
Temperature (°C)	Measurements at Asa and Flakaliden	6.1	2.3
Precipitation (m yr ⁻¹)	Measurements at Asa and Flakaliden	0.736	0.642
Total deposition (mmol _c m ⁻² yr ⁻¹)	Measured data on open field and throughfall deposition available from nearby Swedish ICP Integrated Monitoring Sites	SO ₂ ²⁻ : 27.0 Cl ⁻ : 38.3 NO ₃ ⁻ : 30.7 NH ₄ ⁺ : 21.6 Ca ²⁺ : 7.2 Mg ²⁺ : 6.8 K ⁺ : 1.9 Na ⁺ : 31.5	SO ₂ ²⁻ : 13.1 Cl ⁻ : 5.6 NO ₃ ⁻ : 10.5 NH ₄ ⁺ : 9.9 Ca ²⁺ : 5.2 Mg ²⁺ : 1.9 K ⁺ : 1.1 Na ⁺ : 5.6
Base cation net uptake (mmol _c m ⁻² yr ⁻¹)	Previously measured data for Asa and Flakaliden: Concentrations in biomass from Linder (unpublished data). Biomass data from Heureka simulations.	Ca ²⁺ : 46.2 Mg ²⁺ : 10.6 K ⁺ : 17.8	Ca ²⁺ : 26.7 Mg ²⁺ : 4.4 K ⁺ : 6.7
Net nitrogen uptake (mmol _c m ⁻² yr ⁻¹)	Previously measured data from Asa and Flakaliden: Concentrations in biomass from Linder (unpublished data). Biomass data from Heureka simulations.	81.0	32.4
Base cations in litterfall (mmol _c m ⁻² yr ⁻¹)	Literature data from Hellsten et al. (2013)	Ca ²⁺ : 116.8 Mg ²⁺ : 15.1 K ⁺ : 10.5	Ca ²⁺ : 40.6 Mg ²⁺ : 4.6 K ⁺ : 3.2
Nitrogen in litterfall (mmol _c m ⁻² yr ⁻¹)	Literature data from Hellsten et al. (2013)	179.8	47.5
Evapotranspiration (Fraction)	Precipitation data and runoff data. Runoff data calculated based on proportion of runoff to precipitation (R/P) at Gammtratten and Aneboda.	0.3	0.6

Table 4b. Soil* parameters used in the PROFILE model.

Parameter	Unit	Source
Exposed mineral surface area	m ² m ⁻³	Own measurements used together with Eq. 5.13 in Warfvinge and Sverdrup (1995)
Soil bulk density	kg m ⁻³	Own measurements
Soil moisture	m ³ m ⁻³	Based on paragraph 5.9.5 in Warfvinge and Sverdrup (1995)
Mineral composition	Weight fraction	Own measurements
Dissolved organic carbon	mg L ⁻¹	Previously measured data for Asa and Flakaliden: Measurements for B-horizon from Harald Grip and previously measured data from Fröberg et al. (2013)
Aluminium solubility coefficient	kmol m ⁻³	Own measurements for total organic carbon and oxalate-extractable Al together with function developed from previously published data (Simonsson and Berggren, 1998)
Soil solution CO ₂ partial pressure	atm.	Based on paragraph 5.10.2 in Warfvinge and Sverdrup (1995)

*Physical and chemical soil layer specific input data are given in supplements (Table S3-S4)

988

989

990

991

992

993

994

995

996

997

998

999

1000

1001

1002

1003

1004

1005

1006
 1007
 1008
 1009
 1010
 1011
 1012
 1013
 1014
 1015

Table 5. Judgement of data quality for terms included in the base cation budget estimate of weathering

Term	Spatial scale	Temporal scale	Data source	Quality of term quantification
Deposition	Adjacent sites	Annual or monthly measurements	Svartberget experimental forest, and Integrated Monitoring site	Moderate: high quality of data, but estimates are not site-specific
Soil stock change	Site (initial) and plot (repeated)	Repeated samplings (2)	Unpublished data from J. Bergholm and H. Grip.	Moderate/low: repeated sampling biased by differences in methods of sampling and soil extraction.
Leaching	Plot	Sampling of soil water at 50 cm depth repeated 2 times per year. Water flux modelled (COUP).	H. Grip, unpublished data	High/moderate: High spatial and temporal resolution in soil chemistry, but uncertainty in separating lateral and vertical flow (Flakaliden).
Biomass accumulation	Site (control plots)	Growth increment measured from biomass studies at start and after 12 years.	Growth Albaugh et al. (2009) Nutrient content: S: Linder unpublished data	High/moderate: High quality in growth estimates and nutrient content at treatment scale, data lacking at plot scale

1016
 1017

1018
 1019
 1020
 1021
 1022
 1023
 1024
 1025
 1026
 1027
 1028
 1029
 1030
 1031

Table 6: Standard errors and standard uncertainties ($\text{mmol}_c \text{ m}^{-2} \text{ yr}^{-1}$) for the terms in the base cation budget, Eq. (4). Combined standard uncertainty, plot average value and confidence interval for the weathering rate of base cation i derived from base cation budgets $W_{\text{budget}, i}$ ($\text{mmol}_c \text{ m}^{-2} \text{ yr}^{-1}$).

Site	Element	Deposition	Soil change	Biomass accum.	Leaching	Combined standard uncertainty	W_{budget}	Confidence interval (combined standard uncertainty $\times 3$)
Asa	Ca	1.1	12.9	19.5	3.2	24	58	± 71
	Mg	1.1	0.6	2.5	1.6	3	29	± 10
	K	0.3	1.0	9.7	0.1	10	37	± 29
	Na	4.0	0.9	0.0	5.1	7	7	± 20
Flakaliden	Ca	0.8	10.5	13.3	0.7	17	28	± 51
	Mg	0.3	1.1	1.5	0.3	2	12	± 6
	K	0.2	0.6	6.7	0.2	7	19	± 20
	Na	0.7	1.2	0.0	0.8	2	2	± 5

1032
 1033
 1034
 1035

1036

1037 **Figure captions**

1038 **Figure 1.** Titanium (Ti) to zirconium (Zr) ratio (by concentration) used as an indicator of uniform parent material
1039 in all soil layers at Asa (F3, F4, K1, K4) and Flakaliden (10B, 11B, 14B, 15A).

1040 **Figure 2.** Zirconium (Zr) gradient in the soil at Asa (K1, K4, F3, F4) and Flakaliden (10B, 11B, 14B, 15A)

1041 **Figure 3.** (Left) Historical weathering rate of base cations ($\text{mmol}_c \text{m}^{-2} \text{yr}^{-1}$) estimated by the depletion method
1042 and (right) steady-state weathering rate estimated by the PROFILE model in different soil layers at Asa and
1043 Flakaliden.

1044 **Figure 4.** Comparison of weathering rates ($\text{mmol}_c \text{m}^{-2} \text{yr}^{-1}$) for Ca, Mg, Na and K determined with the depletion
1045 method, the PROFILE model and the base cation budget method for the 0-50 cm layer at Asa and Flakaliden. For
1046 the weathering rates based on the depletion method and the PROFILE model, error bars represent the standard
1047 error calculated based on four soil profiles at each study site, except for Flakaliden, where the depletion method
1048 was only applied in two soil profiles. For weathering rates based on the base cation budget approach, error bars
1049 represent combined standard uncertainties, which are based on standard errors derived from plot-wise replicated
1050 data of the present experiments (for leaching and changes in exchangeable soil pools) and on standard
1051 uncertainties derived from Simonsson et al. 2015, where replicated data were missing in the present study (for
1052 accumulation in biomass and total deposition).

1053 **Figure 5.** (Left) Sinks and (right) sources of base cations in ecosystem net fluxes at Asa and Flakaliden. The soil
1054 is a net source of soil base cation stocks decrease and a net sink if they increase. 'BC budget' = current base cation
1055 weathering rate (W_{budget}) estimated with the base cation budget method, including measured changes in soil
1056 extractable base cation stocks; 'PROFILE' = soil extractable pools estimated from base cation budget using
1057 PROFILE estimates of steady-state weathering rate; 'Historical' = soil extractable pools estimated from base cation
1058 budget using estimates of historical weathering rate by the depletion method. 'Measured soil change' and 'Base
1059 cation budget estimated soil change' indicates that equation 4 was used to estimate weathering rate or the soil
1060 change, respectively.

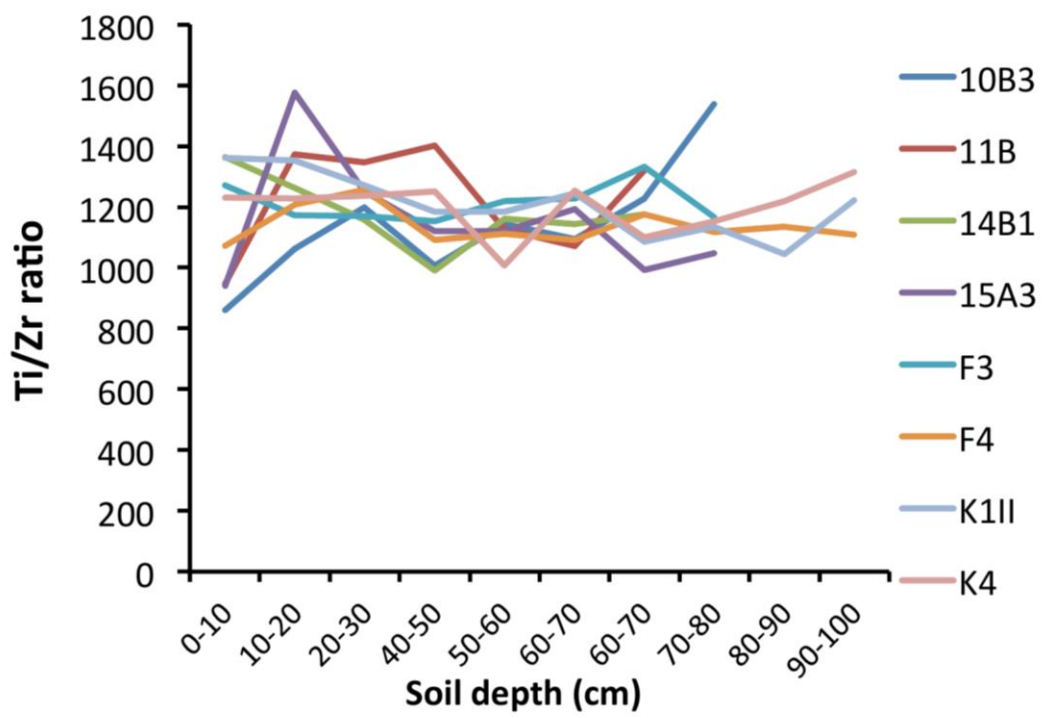
1061 **Figure 6.** Time (years) required to achieve the measured historical element loss in different soil layers with
1062 maximum or minimum PROFILE weathering rates at (a) Flakaliden and (b) Asa.

1063

1064

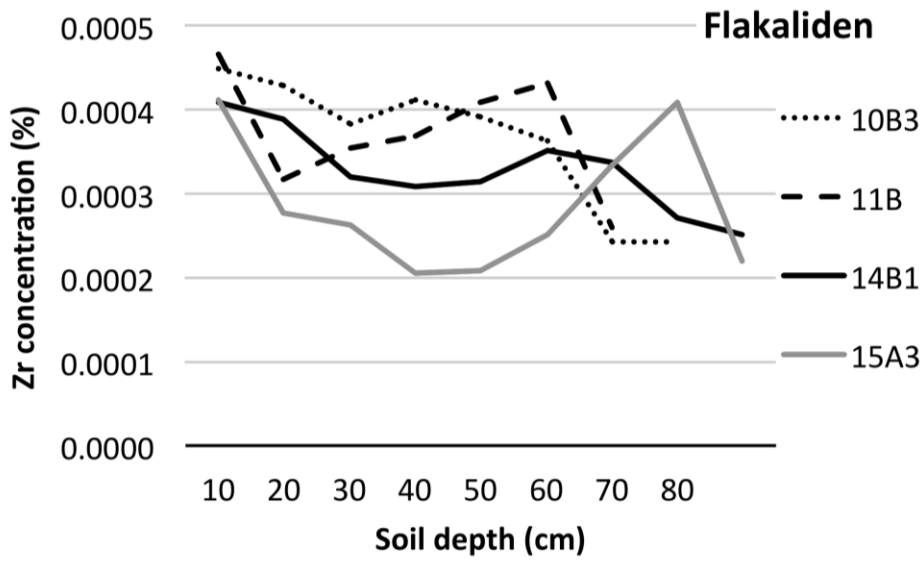
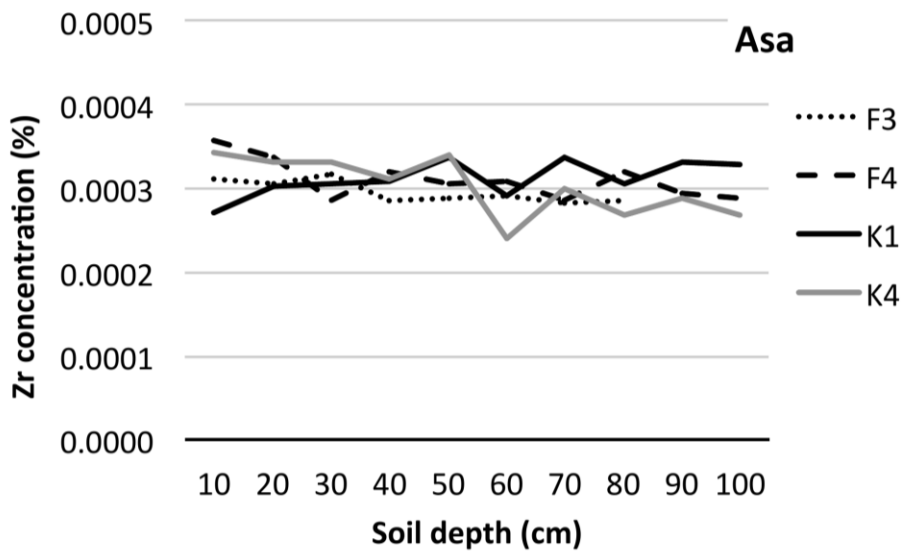
1065

1066
1067
1068
1069
1070
1071
1072
1073
1074

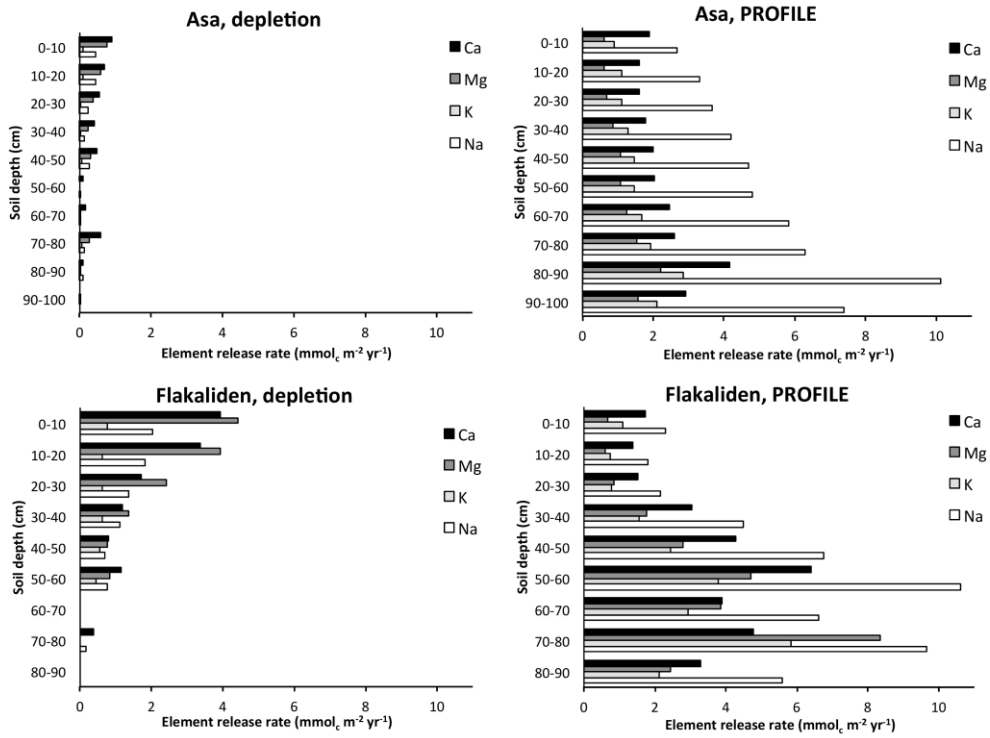


1075
1076
1077
1078

Figure 1.



1079
 1080 Figure 2.
 1081



1082

1083 **Figure 3.**

1084

1085

1086

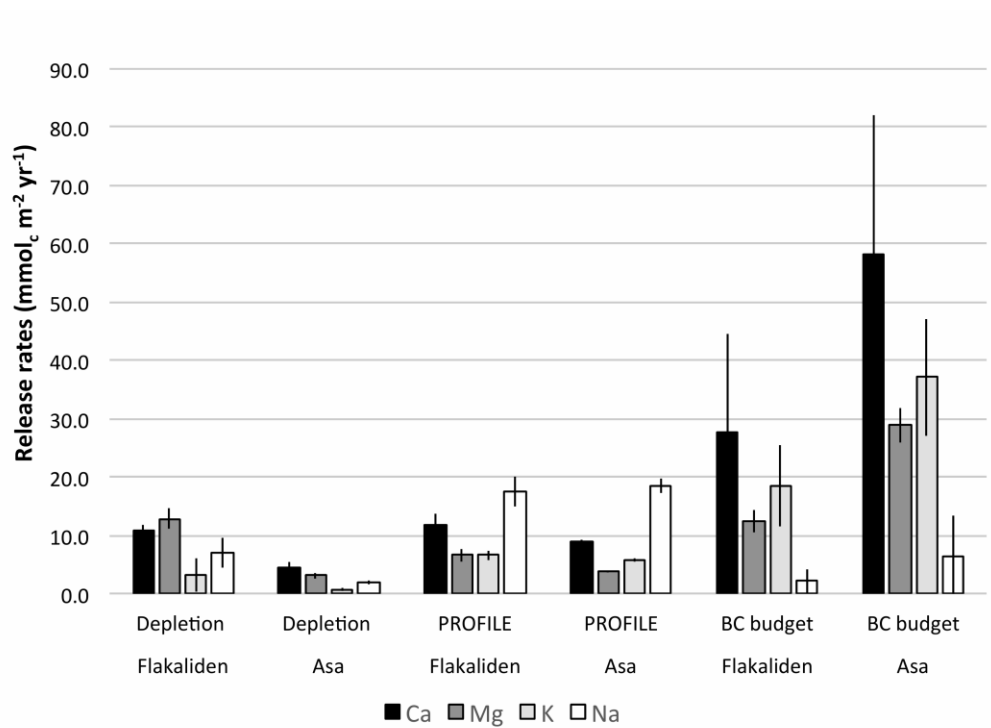
1087

1088

1089

1090

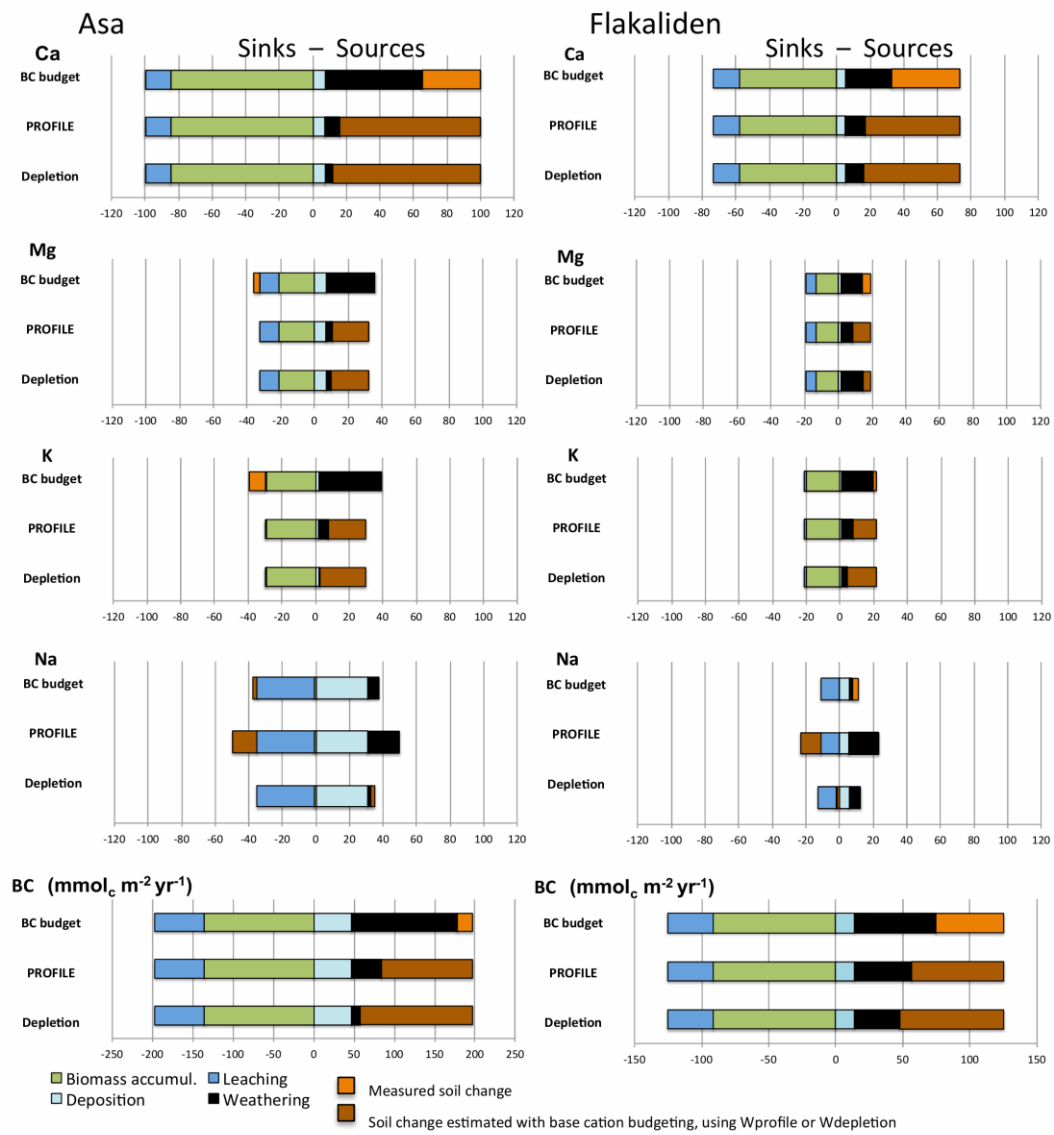
1091



1092

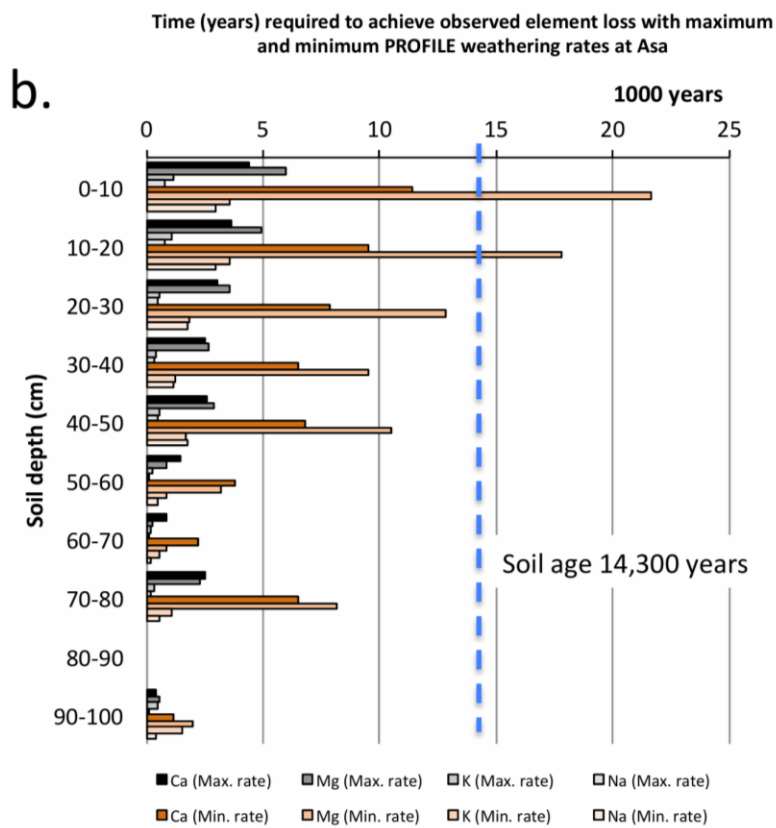
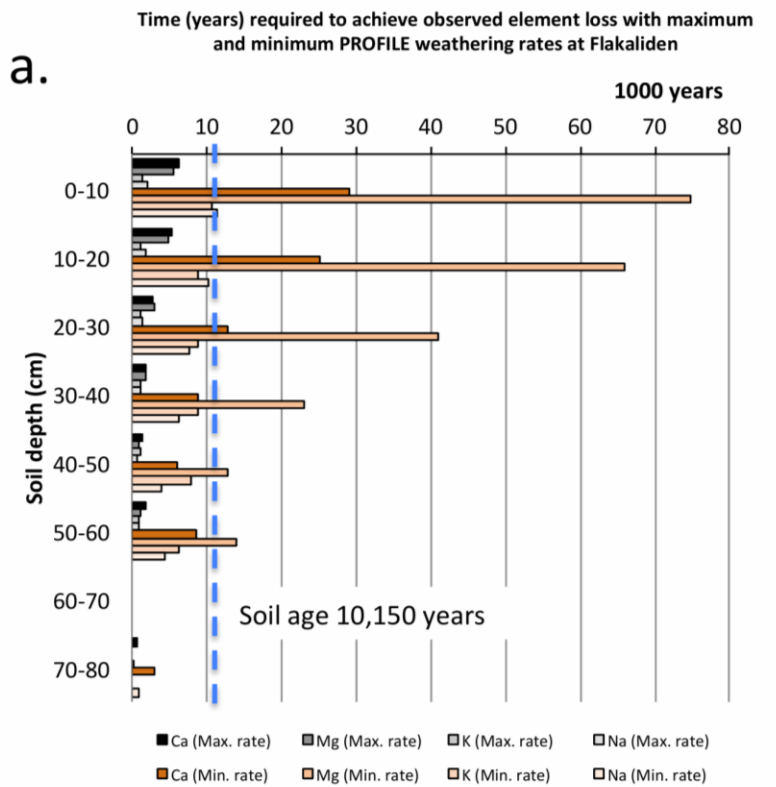
1093 **Figure 4.**

1094



1095

1096 **Figure 5.**



1097
1098
1099

Figure 6.